SRI International

EVALUATION OF A DIFFUSION/TRAPPING MODEL FOR HYDROGEN INGRESS IN HIGH-STRENGTH ALLOYS

Bruce G. Pound, Group Leader
Corrosion Science and Technology

SRI Project PYU-2969

REPORT DOCUMENTATION PAGE

Public reporting burden for this collection of information is estimated to average 1 hour per response, including the time for reviewing instructions, searching existing data sources, gathering and maintaining the data needed, and completing and reviewing the collection of information. Send comments regarding this burden estimate or any other aspect of this collection of information, including suggestions for reducing this burden, to Washington Headquarters Services, Directorate for Information Operations and Reports, 1215 Jefferson Davis Highway, Suite 1204, Arlington, VA 22202-4302, and to the Office of Management and Budget, Paperwork Reduction Project (0704-0188), Washington, DC 20503.

1. AGENCY USE ONLY (Leave blank)	2. REPORT DATE Oct 92	3. REPORT TYPE AND DATES COVERED Final 15 Sept 91-14 Sept 93

4. TITLE AND SUBTITLE
Evaluation of a Diffusion/Trapping Model for Hydrogen Ingress in High-Strength Alloys.

5. FUNDING NUMBERS
N00014-91-C-0263

6. AUTHOR(S)
Bruce G. Pound

7. PERFORMING ORGANIZATION NAME(S) AND ADDRESS(ES)
SRI International
333 Ravenswood Ave.
Menlo Park, CA 94025

8. PERFORMING ORGANIZATION REPORT NUMBER
PYU-2969

9. SPONSORING/MONITORING AGENCY NAME(S) AND ADDRESS(ES)
Office of Naval Research, Code 3312
800 N. Quincy St.
Arlington, VA 22217-5000

10. SPONSORING/MONITORING AGENCY REPORT NUMBER

11. SUPPLEMENTARY NOTES

12a. DISTRIBUTION/AVAILABILITY STATEMENT
Approved for public release - distribution unlimited

12b. DISTRIBUTION CODE

13. ABSTRACT (Maximum 200 words)
Alloys developed to improve strength, weight, and corrosion resistance often remain susceptible to hydrogen embrittlement (HE). The objective of this research was to investigate hydrogen ingress in high performance alloys, particularly in terms of irreversible trapping, with a view to characterizing their susceptibility to HE. A technique referred to as hydrogen ingress analysis by potentiostatic pulsing (HIAPP) was applied to five unaged and aged ß-Ti alloys (Beta-C, Ti-10-2-3, Ti-13-11-3, Ti-15-3, and Beta-21S), an alpha-beta Ti alloy (Ti-6-4), two Cu-Ni alloys (Marinel and Monel K-500), and a Ni-base alloy (UNS N07716). Anodic transients obtained in 1 mol/L HAc-1 mol/L NaAc (Ac = acetate) were analyzed using a diffusion/trapping model to evaluate the trapping constant and hydrogen entry flux. Except for Ti-15-3, aging increases irreversible trapping in the ß-Ti alloys, the increase paralleling the decrease in their tolerance to hydrogen. Ti-13-11-3 is indicated to be the most susceptible to HE, followed by Beta-21S, Beta-C, Ti-10-2-3, and Ti-15-3, with the trapping constants apparently being determined by the degree of grain boundary alpha phase. The trapping constants for aged Marinel and alloy K-500 do not appear to differ significantly, but a lower flux for Marinel accounts, at least partly, for its higher resistance to HE. Likewise, a low flux for alloy 716 is consistent with it generally being resistant to cracking.

14. SUBJECT TERMS
Beta-Titanium Alloys, Monel K-500, Marinel, Alloy 716, Potentiostatic Pulse
Hydrogen Trapping, Trapping Model, Hydrogen Ingress

15. NUMBER OF PAGES
80

16. PRICE CODE

17. SECURITY CLASSIFICATION OF REPORT	18. SECURITY CLASSIFICATION OF THIS PAGE	19. SECURITY CLASSIFICATION OF ABSTRACT	20. LIMITATION OF ABSTRACT
UNCLASSIFIED	UNCLASSIFIED	UNCLASSIFIED	UL

i

CLASSIFIED BY:

DECLASSIFY ON:

CONTENTS

A-11

PREFACE

This final report describes work performed under Office of Naval Research (ONR) Contract No. N00014-91-C-0263 in a continuation of our program to investigate hydrogen ingress into various high performance alloys, particularly in terms of irreversible trapping, with a view to characterizing the susceptibility of the alloys to hydrogen embrittlement (HE). A technique called hydrogen ingress analysis by potentiostatic pulsing (HIAPP) was used to obtain anodic current transients for the alloys in 1 mol L^{-1} HAc/1 mol L^{-1} NaAc (Ac = acetate), and the transients were analyzed using a diffusion/trapping model under interface control conditions to evaluate the trapping constant and hydrogen entry flux in each case.

The report is presented as an Executive Summary followed by five papers that have been submitted to refereed journals or conference proceedings for publication:

1. "The Effect of Aging on Hydrogen Trapping in β-Titanium Alloys," submitted to *Acta Metall. Mater.*

2. "Hydrogen Trapping in β-Titanium Alloys — The Link Between Microstructure and Hydrogen Embrittlement," submitted to *Acta Metall. Mater.*

3. "The Ingress of Hydrogen into Copper-Nickel Alloys," submitted to *Corrosion.*

4. "A Comparison of Hydrogen Ingress Behavior in Alloys 716 and 625," accepted by *Scripta Metall. Mater.*

5. "Predicting the Susceptibility to Hydrogen Embrittlement," in *Proceedings of the 12th International Corrosion Congress, Houston, Texas, September 1993.*

The first two papers cover a group of five β-Ti alloys (Beta-C, Ti-10-2-3, Ti-13-11-3, Beta-21S, and Ti-15-3) and the next two concern a pair of Cu-Ni alloys (Marinel and Monel K-500) and a pair of Ni-base alloys (Custom Age 625 PLUS and Inconel 625). The final paper is a review of HIAPP and its application to various alloys studied during our program with ONR; some of the work reported there was supported by our earlier ONR contract, No. N00014-86-C-0233.

The principal investigator would like to acknowledge the following assistance in this work: Dr. Jacques Giovanola of the Fracture Mechanics Laboratory in SRI's Poulter Laboratory provided samples of Ti-10-2-3 and was available for helpful discussions of the microstructure of the β-Ti alloys. RMI Titanium Co. (Niles, OH) provided samples of Beta-C Ti, Professors R. Gangloff

and J. Scully of the University of Virginia provided samples of Ti-15-3 and Beta-21S Ti, and Langley Alloys, Ltd. (Berkshire, England) provided samples of Marinel.

EXECUTIVE SUMMARY

High performance alloys continue to be developed to improve key properties such as strength, weight, and corrosion resistance, but their susceptibility to hydrogen embrittlement (HE) remains a concern in many situations. The HE susceptibility is strongly influenced by the presence of microstructural heterogeneities, which can provide sites to trap hydrogen. For most alloys, the degradation in mechanical properties caused by hydrogen reflects their intrinsic susceptibility determined by the trapping characteristics. However, the amount of hydrogen entering the alloy can play a critical role in determining whether embrittlement will actually occur. Consequently, alloys should be characterized in terms of both trapping capability and the rate of hydrogen entry to assess their likelihood of embrittlement.

This report describes work performed during a continuation of our program with the Office of Naval Research to investigate hydrogen ingress in various high performance alloys, particularly in terms of irreversible trapping, with a view to characterizing the susceptibility of the alloys to HE. A technique referred to as hydrogen ingress analysis by potentiostatic pulsing (HIAPP) was used to obtain anodic current transients for the alloys in 1 mol L^{-1} HAc/1 mol L^{-1} NaAc (Ac = acetate) containing 15 ppm As$_2$O$_3$. The transients were analyzed using a diffusion/trapping model under interface control conditions to evaluate the apparent trapping constant (k_a) and hydrogen entry flux in each case. Where possible, k_a was then used to determine the irreversible trapping constant (k) and the density of irreversible traps.

The first part of this work focused on investigating the trapping behavior and, where appropriate, identifying the principal irreversible traps of five unaged and aged ß-titanium alloys (Beta-C, Ti-10V-2Fe-3Al, Ti-13V-11Cr-3Al, Ti-15V-3Cr-3Al-3Sn and Beta-21S) and an α-β titanium alloy (Ti-6Al-4V). It was found that, except for Ti-15-3, aging caused a marked increase in irreversible trapping for all the β-Ti alloys, this increase paralleling the reported decrease in their tolerance to hydrogen. The increase in trapping was attributed to precipitation of secondary α phase; that is, the higher k observed for the aged alloys appeared to be associated with irreversible trapping at the α/β interface, presumably in addition to the irreversible trapping occurring at other sites that are also present in the unaged alloys.

A comparison of the trapping constants for the aged β-Ti alloys indicated that Ti-13-11-3 is the most susceptible to HE, followed by Beta-21S, Beta-C, Ti-10-2-3, and then Ti-15-3. The trapping constants for aged Beta-21S and Ti-15-3 are consistent with the relative resistances of

these alloys to HE, as determined in other studies. The low trapping constant for Ti-15-3 in particular matches the high resistance reported for this alloy.

The magnitude of k_a for aged β-Ti alloys appears to be determined by the degree of α precipitation at grain boundaries. The low value of k_a for Ti-15-3 reflects the lack of preferential α precipitation on grain boundaries, whereas the high k_a for aged Beta-21S is apparently indicative of the considerable grain boundary α phase as well as fine intragranular α platelets. The results address the fundamental question of whether yield strength or microstructure has the predominant effect on HE, with the apparent relationship between hydrogen trapping and location of the secondary α phase suggesting that the resistance of aged β-Ti alloys to HE is primarily dependent on microstructure.

The second part of the study involved two Cu-Ni alloys, Marinel and Monel K-500. Aged alloy K-500 was found to have the highest value of k, but the uncertainty in the values of k renders them close enough that any difference in susceptibility of the aged alloys cannot be distinguished. On the other hand, the hydrogen entry flux for Marinel is clearly lower than that for alloy K-500, the implication being that the local concentration of hydrogen in Marinel should build up more slowly to some critical level. Since the difference in HE behavior of Marinel and alloy K-500 does not appear to be clearly attributable to irreversible trapping, the lower entry flux for Marinel must account, at least partly, for the higher resistance to HE observed for this alloy.

The primary irreversible traps in the two Cu-Ni alloys are believed to involve sulfur and phosphorus segregated at grain boundaries, but a lack of data for grain boundary concentrations precludes verification in terms of calculated trap densities. However, the trap densities for Marinel and alloy K-500 can be correlated with their sulfur and phosphorus levels, which supports the assumption that these species provide the primary irreversible traps.

The final part of the work addressed a Ni-base alloy (Custom Age 625 PLUS designated as UNS N07716). Alloy 716, like alloy 625, is characterized by a single type of irreversible trap. The calculated trap density indicated that the principal irreversible traps are Ti-rich carbide particles. Alloy 716 has the highest irreversible trapping constant among a range of nickel-base alloys, which indicates that it should be the most susceptible to HE. However, the entry flux for alloy 716, as with alloy 625, is apparently low enough that the alloy generally does not undergo cracking during exposure in aggressive environments for up to 1000 h, despite the high susceptibility imparted by the type of traps present.

THE EFFECT OF AGING ON HYDROGEN TRAPPING IN β-TITANIUM ALLOYS

ABSTRACT

The ingress of hydrogen in three β-titanium alloys (Beta-C, Ti-10V-2Fe-3Al, and Ti-13V-11Cr-3Al) and an α-β titanium alloy (Ti-6Al-4V) was investigated with a view to characterizing their interaction with hydrogen. A technique referred to as hydrogen ingress analysis by potentiostatic pulsing (HIAPP) was used to obtain anodic current transients for the unaged and aged β-Ti alloys and as-received Ti-6-4 in an acetate buffer (1 mol L^{-1} HAc/1 mol L^{-1} NaAc, where Ac = acetate). The transients were analyzed using a diffusion/trapping model under interface control conditions to evaluate the trapping constants and hydrogen entry flux in each case. A marked increase in irreversible trapping was observed for the β-titanium alloys with aging and was attributed to precipitation of secondary α phase. Aging also induced changes in the passive film and hence the hydrogen entry flux. Ti-13-11-3 and Ti-10-2-3 are predicted to become less resistant to hydrogen embrittlement with aging as a result of increases in both the trapping constant (at least for Ti-13-11-3) and the flux. In contrast, the change in resistance of Beta-C Ti with aging is subject to the opposing effects of a reduced flux and an enhanced trapping capability, so it is unclear whether aged Beta-C Ti should be less resistant to hydrogen embrittlement than the unaged alloy.

INTRODUCTION

High-performance alloys are increasingly in demand as improved levels of strength, weight, and corrosion resistance are required in various applications. As a result of these requirements, β-titanium alloys, which can be aged to yield strengths in the region of 1200 MPa or higher, have attracted interest as lightweight materials for airframe components subject to high stresses. Most hydrogen embrittlement (HE) studies of titanium alloys have focused on the α–β type, and relatively little work has involved β alloys. Nevertheless, β-Ti alloys, despite their high solubility of hydrogen [1,2], have been found to undergo a loss in ductility. Clearly, the propensity of these alloys to HE needs to be better understood.

The susceptibility of alloys to HE is strongly affected by the interaction of hydrogen with microstructural heterogeneities that act as hydrogen traps. In particular, traps with a large saturability and a high binding energy for hydrogen are regarded as highly conducive to HE.

Consequently, characterization of alloys in terms of such traps can assist in determining their susceptibility to embrittlement.

The entry and trapping of hydrogen in a range of high-strength alloys have been investigated in previous work [3-7] by using a technique referred to as hydrogen ingress analysis by potentiostatic pulsing (HIAPP). As the name indicates, the alloy of interest is subjected to a potentiostatic pulse and the resulting current transients are analyzed in terms of a model for hydrogen diffusion and trapping [3,8,9]. HIAPP has previously been applied to high-strength steels [3-5], precipitation-hardened and work-hardened nickel-base alloys [3-6], and titanium [7] and was shown to be effective in evaluating the trapping characteristics of alloys containing both single and multiple principal traps. The results showed that a range of microstructural features can be identified as the principal irreversible (high binding energy) traps and thus demonstrated the ability of HIAPP to provide a basis for explaining differences in the resistance of alloys to HE. Perhaps more important, it was established that the irreversible trapping constants for the alloys studied can be correlated with their observed resistances to HE.

During the present work, the use of HIAPP was extended to three ß-titanium alloys—Beta-C, Ti-10V-2Fe-3Al (commonly referred to as Ti-10-2-3), and Ti-13V-11Cr-3Al (Ti-13-11-3) — and an α-β titanium alloy, Ti-6Al-4V (Ti-6-4). The objective was to determine the hydrogen ingress behavior of the individual alloys, particularly in terms of irreversible trapping, with a view to characterizing their susceptibility to HE.

EXPERIMENTAL PROCEDURE

Alloys

The composition of each alloy was provided by the producer and is given in Table 1. The Ti-10-2-3 alloy was supplied as an α-β finish-rolled plate (25 mm thick) that was subsequently solution treated at 820°C for 1 h, water quenched, and, where required, aged at 560°C for 1 h in a salt bath. The β-solution (820°C) treatment produced a microstructure that was devoid of primary α phase. However, aging resulted in the precipitation of a fine secondary α phase within the grains and at the grain boundaries. The grain size varied between approximately 50 and 300 μm. The aged material had a yield strength of 1372 MPa. Rods 1.27 cm in diameter were machined from the heat treated plate for use as electrodes. The alloy was used in both the unaged and aged conditions to determine the effect of the secondary α phase on hydrogen ingress.

The Beta-C alloy was supplied as rod that had been hot-rolled, annealed, and centerless ground. The diameter of the rod was 1.593 cm. The yield strength of the as-received (unaged) alloy was given as 864-878 MPa. A section of rod was aged (secondary α precipitated) at 510°C

for 20 h and air cooled to produce a yield strength of 1208-1223 MPa. This alloy was also tested in both the unaged and aged conditions. The Beta-C Ti and Ti-10-2-3 were found to have submicron-sized particles (typically 0.3-0.4 μm in diameter) that appeared to contain varying amounts of Si, S, and P; other workers [10] have reported that Ti(PSSi) inclusions ≤1 μm in diameter are common to Ti-10-2-3 and most other β-Ti alloys.

The Ti-13-11-3 alloy was supplied as cold drawn rod with a diameter of 0.953 cm. Although the alloy is usually solution-treated at various stages during drawing [11], optical micrographs of the Ti-13-11-3 revealed the presence of stress-induced plates, which have been found in solute-rich Ti-V alloys and are considered to be deformation twins [12,13]. A section of rod was aged at 427°C for 10 h and air-cooled to produce a yield strength of 1310-1379 MPa. As with the other two alloys, Ti-13-11-3 was tested in the unaged and aged conditions to establish the role of the secondary α phase precipitated during aging.

The α-β alloy (Ti-6-4) was produced as rod with a diameter of 1.27 cm and was used in the as-received condition. Its yield strength was 1027 MPa.

Technique

Details of the electrochemical cell and instrumentation have been given previously [3]. The test electrodes of each alloy consisted of a length (1.3-3.8 cm) of rod press-fitted into a Teflon sheath so that only the planar end surface was exposed to the electrolyte. The surface was polished before each experiment with SiC paper followed by 0.05-μm alumina powder. The electrolyte was an acetate buffer (1 mol L^{-1} acetic acid/1 mol L^{-1} sodium acetate) containing 15 ppm As$_2$O$_3$ as a hydrogen entry promoter. The electrolyte was deaerated with argon for 1 h before measurements began and throughout data acquisition. The potentials were measured with respect to a saturated calomel electrode (SCE). All tests were performed at 22 ± 1°C.

The test electrode was charged with hydrogen at a constant potential E_c for a time t_c, after which the potential was stepped in the positive direction to a value 10 mV negative of the open-circuit potential E_{oc} [3,8,9]. Anodic current transients with a charge q_a were obtained over a range of charging times (5-60 s) at different overpotentials ($\eta = E_c - E_{oc}$). The open-circuit potential of the test electrode was sampled immediately before each charging time and was also used to monitor the stability of the surface oxide.

ANALYSIS

Diffusion/Trapping Model

The anodic current transients were examined in terms of a diffusion/trapping model [3,8] based on interface-limited diffusion control (referred to simply as interface control). Under these conditions, the rate of hydrogen ingress in an alloy is controlled by diffusion but the entry flux of hydrogen across the interface is restricted; in the case of pure diffusion control, hydrogen entry is assumed to be fast enough that equilibrium is rapidly achieved between adsorbed and subsurface hydrogen. According to the interface control model, the total charge passed out is given in nondimensional form by

$$Q'(\infty) = R^{1/2}\{1 - e^{-R}/(\pi R)^{1/2} - [1 - 1/(2R)]\text{erf}(R^{1/2})\} \tag{1}$$

The nondimensional terms are defined by $Q = q/[FJ(t_c/k_a)^{1/2}]$ and $R = k_a t_c$, where q is the dimensionalized charge in C cm^{-2}, F is the Faraday constant, and J is the ingress flux in mol cm^{-2} s^{-1}. The charge $q'(\infty)$ corresponding to $Q'(\infty)$ is equated to q_a; the adsorbed charge is almost invariably found to be negligible, and so q_a can be associated entirely with absorbed hydrogen. k_a is an apparent trapping constant measured for irreversible traps in the presence of reversible traps and can be expressed by $k(D_a/D_L)$ where k is the irreversible trapping constant, D_a is the apparent diffusivity, and D_L is the lattice diffusivity of hydrogen in the metal.

In all cases except unaged Ti-10-2-3 (discussed below), Eq. (1) could be fitted to data for q_a to obtain values of k_a and J such that J was constant over the range of charging times and k_a was essentially independent of charging potential, as is required for the model to be valid. The values of k_a and J can be used to calculate the irreversibly trapped charge (q_T) given nondimensionally by

$$Q_T = [R^{1/2} - 1/(2R^{1/2})]\text{erf}(R^{1/2}) + e^{-R}/\pi^{1/2} \tag{2}$$

The charge associated with the entry of hydrogen into the metal (q_{in}) can be determined from $q_{in} = FJt_c$, and so the trapping efficiency, q_T/q_{in}, can be found.

The density of particles or defects (N_i) providing irreversible traps can be obtained from the apparent trapping constant by using a model [5,9] based on spherical traps:

$$N_i = k_a a/(4\pi d^2 D_a) \tag{3}$$

where a is the diameter of the metal atom and d is the trap radius, which is estimated from the dimensions of heterogeneities that are potential irreversible traps. The value of a for an alloy is taken as the mean of the atomic diameters weighted in accordance with the atomic fraction of each element. Trap densities are calculated for appropriate values of d, so that the predominant irreversible trap can be identified by comparing the values of N_i with the actual concentrations of specific heterogeneities in the alloy.

The assumption of spherical traps in the above model is an approximation in most cases. However, for alloys studied previously, the calculated trap densities have shown close agreement with the concentrations of potential trap particles that are clearly not spherical, which suggests that the use of a more applicable trap geometry would make little difference in identifying the principal traps.

Ti-10V-2Fe-3Al

The anodic charge for unaged Ti-10-2-3 did not vary significantly with t_c, and so k_a could not be determined. The invariance in q_a implies that negligible hydrogen enters the unaged alloy, so q_{in} is approximately zero, and therefore q_a corresponds almost entirely to oxidation of *ad*sorbed hydrogen.

Aged Ti-10-2-3, in contrast to the unaged alloy, did exhibit a dependence of q_a on t_c, so trapping constants could be evaluated in this case. Values of k_a and J for six tests are shown in Table 2. Although k_a was essentially independent of charging potential, it did show some variation between tests. This variation is attributed to differences in the amount of α phase at grain boundaries accessible to hydrogen, the differences resulting from the variation in grain size (50-300 μm). The mean value of k_a for all the tests is 0.066 ± 0.009 s^{-1}. As would be expected for the diffusion/trapping model, the flux increases with potential because of its dependence on the surface coverage of adsorbed hydrogen.

Beta-C Ti

The open-circuit potentials for the aged alloy were typically 200-300 mV more negative than those for the unaged alloy. Hence, the charging potential (E_c) for the aged alloy was correspondingly more negative at a given overpotential. Nevertheless, the values of q_a at the same overpotential were typically 2 to 4 times smaller than those for the unaged alloy. The smaller values of q_a for the aged alloy, as discussed below, resulted from both a decrease in the amount of hydrogen absorbed and an increase in the proportion of the absorbed hydrogen being trapped.

Thus, aging produces two opposing effects in terms of HE: the apparent change in the passive film (as reflected by E_{oc}) reduces hydrogen entry, whereas precipitation of secondary α phase appears to be the likely cause of the enhanced trapping capability. Interestingly, the change in hydrogen absorption induced by aging Beta-C Ti is the reverse of that found for Ti-10-2-3.

The variation in q_a with charging time for Beta-C Ti was considerably less pronounced for the aged alloy; this effect is also due to the smaller amount of absorbed hydrogen and particularly to the increase in trapping capability, as shown below. The smaller variation in q_a for aged Beta-C Ti — and also for aged Ti-13-11-3 (discussed below) — is probably responsible for the greater scatter observed in the trapping constants for these alloys in a particular test. Values of k_a and J for two tests on both the unaged and aged Beta-C alloy are given in Table 3. In both cases, k_a was independent of charging potential, although some scatter, as noted above, occurred with the aged alloy. The overall mean values of k_a for the unaged and aged alloys were 0.031 ± 0.002 s^{-1} and 0.088 ± 0.010 s^{-1}, respectively. As with Ti-10-2-3, the entry flux showed the expected increase with potential for both conditions of the alloy, but it was decreased by aging.

Values of q_{in}, q_T, and q_T/q_{in} calculated using the results for k_a and J at $\eta = -0.45$ V are shown in Figs. 1 (q_{in} and q_T) and 2 (q_T/q_{in}). As to be expected, the decrease in J produced by aging causes a marked decrease in q_{in}, but the corresponding decrease in q_T is lessened because of the higher k_a for the aged alloy. The effect of k_a alone without J can be examined by considering the trapping efficiency (q_T/q_{in}), and it is clear from Fig. 2 that the proportion of hydrogen trapped is greater for the aged alloy. The data for q_T/q_{in} are independent of potential, since each charge component has the same dependence on flux.

The charge (q_a) consumed during hydrogen egress is simply the difference between q_{in} and q_T, and so, as noted above, the changes in q_a with aging can readily be attributed to the changes in J and k_a. The difference, $q_{in} - q_T$, can be expanded to yield

$$q_a = FJ[t_c - (t_c/k_a)^{1/2}Q_T] \tag{4}$$

where Q_T is a multiterm function of k_a and t_c [Eq. (2)], and so it is not obvious whether the decrease observed in q_a for Beta-C Ti is caused primarily by the decrease in J or the increase in k_a. However, the individual effects of J and k_a can be examined by calculating q_a from Eq. (4) for different cases. The variation in q_a with t_c for $\eta = -0.45$ V is shown in Fig. 3. Calculated values for the unaged and aged alloys are represented by the top and bottom curves (1 and 4), respectively, whereas the two middle curves (2 and 3) are hybrids of these cases. It is apparent that the decrease in q_a is somewhat greater with an increase in k_a (curve 3) than with a decrease in J

(curve 2). Moreover, the higher k_a appears to be primarily responsible for restricting the increase in q_a with t_c; that is, the curve tends to flatten as k_a becomes larger.

Ti-13V-11Cr-3Al

In this case, the open-circuit potentials for the aged alloy were typically 400-500 mV more negative than those for the unaged alloy. In addition, the values of q_a were relatively small (<0.05 mC cm^{-2}) for unaged Ti-13-11-3, and — unlike the situation with Beta-C Ti — they were smaller than those for the aged alloy at higher overpotentials (-0.50 to -0.60 V). Nevertheless, even at η = -0.60 V, the unaged and aged alloys differed in q_a by a factor of less than 3.

The increase in q_a with aging suggests that the amount of hydrogen entering the aged alloy exceeds that lost to additional trapping introduced by the secondary α phase. In the case of aged Ti-13-11-3, the change in q_a with charging time was very small and poorly defined within the precision of the data, so only rough values could be estimated for k_a and J. The unaged alloy showed a slightly greater increase in q_a, such that more reliable values of k_a and J could be obtained in this case. Nevertheless, the change in q_a was still modest, with the result that the trapping constants were subject to some scatter.

Values of k_a and J for two tests on both the unaged and aged alloy are shown in Table 4. In both cases, k_a appeared to be independent of charging potential, despite the sizable scatter in some tests for the unaged alloy and the uncertainty in fitting the experimental data for the aged alloy. The overall mean values of k_a for unaged and aged Ti-13-11-3 were 0.069 ± 0.011 s^{-1} and 0.15 ± 0.01 s^{-1}, respectively.

The flux showed the expected increase with potential in both cases and, as with Ti-10-2-3, increased with aging; in essence, unaged Ti-10-2-3 represents a limiting case in that hydrogen ingress is evidently so slow as to be negligible. In the case of Ti-13-11-3, the increase in flux with aging may have resulted from the considerably more negative charging potentials used for the aged alloy. On the other hand, the charging potentials for unaged and aged Ti-10-2-3 differed much less (typically <150 mV at each overpotential) than those for Ti-13-11-3, and yet aging appears to induce a similar marked effect on hydrogen entry for both alloys. Hence, the increase in flux with aging for Ti-10-2-3 and Ti-13-11-3 may have resulted at least partly from changes in the passive film.

The variation in q_a calculated using the values of k_a and J at η = -0.55 V is shown in Fig. 4. The top and middle curves (1 and 2) represent data for the aged and unaged alloys, respectively, whereas curve 3 corresponds to the aged condition but with J limited to that for an

unaged surface. The increase in k_a without a change in J (curve 3), as noted above, acts to decrease not only q_a but also its dependence on t_c. The principal effect of a higher J on curve 3 is to raise q_a, resulting in curve 1 for the aged alloy.

Ti-6Al-4V

Values of k_a and J for two tests on this as-received alloy are shown in Table 5. As with the β-Ti alloys, k_a is essentially independent of charging potential, and the flux increases with potential. The mean value of k_a for both tests was 0.063 ± 0.005 s^{-1}.

DISCUSSION

Irreversible Trapping Constants

The mean values of the trapping constants for the β-titanium alloys and Ti-6-4 are summarized in Table 6. Also shown are data obtained for titanium grade 2 in previous work using HLAPP [7]. The irreversible trapping constant (k) can be derived from k_a by using diffusivity data for the "pure" alloy to obtain the lattice diffusivity (D_L) and for the actual alloy to obtain the apparent diffusivity (D_a). The "pure" alloy is considered to be Ti with its principal alloying elements, so that minor elements are assumed to be primarily responsible for reversible trapping in the actual alloys.

The role of defects such as vacancies and edge dislocations in reversible trapping should also be considered, but their effect can be treated as secondary on the basis of a comparison of hydrogen transport in other metals. Whereas the lattice diffusivity of hydrogen in iron is high enough to be affected by reversible trapping, the transport of hydrogen in fcc metals appears to be limited by diffusion itself, with little hindrance from defects such as vacancies or edge dislocations [14]. The diffusivities for β-Ti alloys at 25°C are intermediate between those for iron and nickel; for example, the diffusivity for Ti-13-11-3 is 2.7×10^{-11} m^2 s^{-1} at 25°C [15], whereas the corresponding values for iron [16,17] and nickel [18,19] are on the order of 10^{-9} and 10^{-14} m^2 s^{-1}, respectively. In addition, the diffusivities for β-Ti alloys are comparable with that for palladium (1-4.5×10^{-11} m^2 s^{-1}) [16,20-23], for which reversible trapping apparently has little effect (since the diffusivity is similar for annealed and unannealed palladium). Hence, the diffusivities for β-Ti alloys appear to be low enough that reversible trapping at defects can be ignored.

In the case of Ti grade 2, the irreversible trapping constant can be approximated to the apparent trapping constant on the basis of the low diffusivity of hydrogen in α-Ti (1.65×10^{-16} m^2 s^{-1} at 25°C) [24] and the closeness in the composition of the grade 2 metal and pure titanium.

Because of these factors, the diffusivities for the pure and commercial grades are assumed to differ negligibly, so that $D_a \approx D_L$ and therefore $k \approx k_a$.

The situation regarding D_a is more debatable for the β-titanium alloys. Few data are available in the literature for the diffusivity of hydrogen in these alloys, with or without minor alloying elements. As a rough approximation, the minor elements in the β-Ti alloys also can be assumed to contribute only slightly to reversible trapping for diffusivities on the order of 10^{-11} m^2 s^{-1}. In effect, this assumption allows a lower limit to be determined for k in each case (Table 6), since trapping invariably causes $D_a < D_L$ and therefore $k > k_a$.

Effect of Aging

Commercial β-Ti alloys such as Ti-10-2-3 and Beta-C contain as much as 60% α phase in their optimally heat-treated conditions. The presence of the α phase increases the possibility of hydride formation either in the α phase or at the α/β interface [25]. In α-β Ti alloys, hydrogen segregates to the interface between the two phases and forms brittle hydrides at these sites, with growth occurring preferentially into the α phase [26]. The tendency to hydride formation is expected to decrease as the volume fraction of the β phase increases, and therefore β alloys should be less prone to hydride induced embrittlement than near-α or α-β alloys.

Various studies do indeed indicate that HE of fully β-phase Ti alloys is not associated with hydride precipitation. For example, Ti-20V suffers a loss of ductility when exposed to hydrogen, but no hydrides are apparent except possibly at very high levels of hydrogen [1]. Likewise, annealed, fully β-phase Ti-13-11-3 can be embrittled without forming detectable hydride platelets [2]. Accordingly, a pronounced difference in the trapping characteristics of unaged and aged β-Ti alloys should be observable.

Irreversible trapping constants were evaluated, as described above, for both the unaged and aged β-titanium alloys studied in this work. Although the values shown in Table 6 represent lower limits, the results indicate clearly that k increases markedly with aging, paralleling the reported decrease in tolerance to hydrogen [27]. The additional trapping is undoubtedly associated with the secondary α phase precipitated during aging, which has been discussed in detail elsewhere [13].

Coupled with the evidence [26] concerning hydride sites, the higher k for the aged alloys suggests that irreversible trapping occurs at the α/β interface, presumably in addition to the irreversible trapping occurring at other sites that are also present in the unaged alloys. Irreversible trapping at the α/β interface, and possibly in the α phase if hydrides grow in from the interface, implies that any diffusion of hydrogen through non-hydrided α phase should be negligible. The α phase should therefore have little influence on the diffusivity in terms of reversible trapping, and so

1-9

D_a is considered to have the same value for the aged and unaged conditions. Furthermore, D_L should also differ little between the two conditions. Hence, the values of k (or k_a) for an unaged and aged alloy can be compared despite the lack of diffusivity data.

The trapping character of unaged and aged Beta-C Ti is consistent with the somewhat equivocal results of sustained load tests on cathodically charged notched tensile specimens [28]. The load tests showed that solution-treated but unaged Beta-C Ti did not crack during exposure for 720 h (30 days), whereas solution-treated and aged alloy cracked after 175 h. However, the cracking behavior was compared in terms of percent of yield strength, so the applied stress was different for the two conditions, making it uncertain whether stress level or microstructure was the controlling factor. The aged alloy may not have cracked at the stress level of the unaged specimen. Nevertheless, it was argued [28] that, if hydrides were involved, the aged Beta-C Ti with its α phase should be more susceptible to HE than the unaged alloy, as indeed indicated by the trapping constants.

Aging was also found to affect the passive film and therefore the hydrogen entry flux. In the case of Ti-13-11-3 and Ti-10-2-3, J increases with aging. Hence, these two alloys are predicted to become less resistant to HE with aging as a result of increases in both the trapping constant (at least for Ti-13-11-3) and the flux. In contrast, aging Beta-C Ti induces a considerable decrease in J, so the change in resistance in this case is subject to two opposing effects — a reduction in the flux and an enhanced trapping capability. As a result, it is uncertain whether aged Beta-C Ti should be less resistant to HE than the unaged alloy, since the increase in k reflects a higher intrinsic susceptibility whereas the decrease in J implies that there is less likelihood of embrittlement actually occurring during a specific period of exposure.

Identification of Irreversible Traps in Unaged Alloys

In the absence of α phase, the trapping constants must be interpreted in terms of some other microstructural feature(s). In Ti grade 2, interstitial nitrogen is thought to be the principal irreversible trap at low hydrogen levels [7]. However, the density of traps calculated from k_a [Eq. (3)] on the basis of nitrogen suggests that a different type of trap predominates in unaged β-Ti alloys. In the case of Beta-C Ti, for example, using $D_a = 3 \times 10^{-11}$ m^2 s^{-1} (the D_a value was assumed to be similar to that for Ti-13-11-3), $d = 74 \times 10^{-12}$ m, and $a = 285 \times 10^{-12}$ m gave a value of 4.3×10^{18} m^{-3} for N_i, whereas the actual nitrogen content (0.018 wt%) in the alloy corresponded to a concentration of 6.5×10^{25} atoms m^{-3}.

Our previous studies [3-6] using HIAPP have shown that nonmetallic inclusions and precipitates are generally the predominant irreversible traps in iron- and nickel-base alloys. Hence,

1-10

the submicron-sized (~0.3-0.4 μm) particles — probably Ti(PSSi) — observed in the unaged Beta-C and Ti-10-2-3 must be considered as possibilities for the principal irreversible traps. However, when the mean trap radius was taken as 0.2 μm and the above values for D_a and a used in the case of Beta-C, N_i was calculated to be 6×10^{11} m^{-3}, compared with about 10^{16} m^{-3} for the actual concentration of particles. Clearly, these particles do not appear to be the principal irreversible traps in the unaged alloys.

At this stage, the principal traps remain unidentified. Other potential traps include grain boundaries and β flecks, which are regions containing higher volume fractions of β phase [13]. The interaction of hydrogen with such regions is expected to be comparable to that with intermetallic precipitates in alloys such as 18Ni maraging steel, so it probably takes the form of reversible trapping [5,29]. Hence, grain boundaries are considered to be the most likely sites for irreversible trapping in unaged β-Ti alloys.

SUMMARY

The ingress of hydrogen in three β-titanium alloys (Beta-C, Ti-10V-2Fe-3Al, and Ti-13V-11Cr-3Al) and an α-β titanium alloy (Ti-6Al-4V) can be analyzed using a diffusion/trapping model under interface control conditions. The principal findings are summarized as follows:

- Only a lower limit could be determined for the irreversible trapping constant (k) in each case, but the results indicated clearly that k increases markedly with aging. The higher k for the aged alloys appears to be associated with irreversible trapping at the α/β interface, presumably in addition to the irreversible trapping occurring at other sites that are also present in the unaged alloys.

- The trapping constants for unaged and aged Beta-C Ti are consistent with the relative resistances to HE as indicated (albeit with some question) by the results of sustained load tests.

- Aging also affects the passive film and therefore the hydrogen entry flux. For Ti-13-11-3 and Ti-10-2-3, J is found to increase, whereas it decreases for Beta-C Ti. In the case of unaged Ti-10-2-3, hydrogen ingress is evidently so slow as to be negligible, and therefore k_a and J could not evaluated.

- Ti-13-11-3 and Ti-10-2-3 are predicted to become less resistant to HE with aging as a result of increases in both the trapping constant (at least for Ti-13-11-3) and the flux. In contrast, the change in resistance of Beta-C Ti is subject to two opposing effects — a reduction in the flux and an enhanced trapping capability— so it is uncertain whether aged Beta-C Ti should be less resistant to HE than the unaged alloy.

- The principal irreversible trap in unaged β-Ti alloys does not appear to be interstitial nitrogen, as is thought to be case for Ti grade 2 at low hydrogen levels. Submicron-sized particles, which are probably Ti(PSSi), can also be discounted, leaving grain boundaries as the most likely sites for irreversible trapping in unaged β-Ti alloys.

ACKNOWLEDGEMENTS

REFERENCES

1. N. E. Paton, R. A. Spurling, and C. G. Rhodes, in *Hydrogen Effects in Metals: Proceedings of the Third International Conference on the Effect of Hydrogen on Behavior of Materials,* Moran, Wyoming, 1980, I. M. Bernstein and A. W. Thompson, Eds., (The Metallurgical Society of AIME, Warrendale, Pennsylvania, 1981), p. 269.

2. P. A. Blanchard, R. J. Quigg, F. W. Schaller, E. A. Steigerwald, and A. R. Troiano, WADC Technical Report 59-172, Wright-Patterson Air Force Base, Ohio (April, 1959); cited in Ref. 15.

3 B. G. Pound, Corrosion **45**, 18 (1989).

4. B. G. Pound, Corrosion **46**, 50 (1990).

5. B. G. Pound, Acta Metall. **38**, 2373 (1990).

6. B. G. Pound, Acta Metall. **39**, 2099 (1991).

7. B. G. Pound, Corrosion **47**, 99 (1991).

8. R. McKibbin, D. A. Harrington, B. G. Pound, R. M. Sharp, and G. A. Wright, Acta Metall. **35**, 253 (1987).

9. B. G. Pound, R. M. Sharp, and G. A. Wright, Acta Metall. **35**, 263 (1987).

10. T. W. Duerig, G. T. Terlinde, and J. C. Williams, Metall. Trans. **11A**, 1987 (1980).

11. D. Warmuth, Astro Metallurgical, personal communication (1992).

12. M. Oka and Y. Taniguchi, Metall. Trans. **10A**, 651 (1979).

13. T. W. Duerig and J. C. Williams, in *Beta Titanium Alloys in the 1980's*, R. R. Boyer and H. W. Rosenberg, Eds. (The Metallurgical Society of AIME, Warrendale, Pennsylvania, 1984), p. 19.

14. W. D. Wilson and S. C. Keeton, in *Advanced Techniques for Characterizing Hydrogen in Metals*, N. F. Fiore and B. J. Berkowitz, Eds. (The Metallurgical Society of AIME, Warrendale, Pennsylvania, 1981), p. 3.

15. W. R. Holman, R. W. Crawford, and F. Paredes, Jr., Trans. Met. Soc. AIME **233**, 1836 (1965).

16. J. Bowker and G. R. Piercy, Metall. Trans. **16A**, 715 (1985)

17. A. J. Kumnick and H. H. Johnson, Metall. Trans. **5**, 1199 (1974).

18. R. M. Latanision and M. Kurkela, Corrosion **39**, 174 (1983).

19. A. M. Brass, A. Chanfreau, and J. Chêne, in *Hydrogen Effects on Material Behavior*, N. R. Moody and A. W. Thompson, Eds. (The Minerals, Metals, and Materials Society, Warrendale, Pennsylvania, 1990), p. 19.

20. M.A.V. Devanathan and Z. Stachurski, Proc. R. Soc. London, Ser. A **270**, 90 (1962).

21. M. Fullenwider, J. Electrochem. Soc. **122**, 648 (1975).

22. J. G. Early, Acta Metall. **26**, 1215 (1978).

23. V. Breger and E. Gileadi, Electrochim. Acta **16**, 177 (1971).

24. I. I. Phillips, P. Poole, and L. L. Shreir, Corros. Sci. **14**, 533 (1974).

25. J. E. Costa, D. Banerjee, and J. C. Williams, in *Beta Titanium Alloys in the 1980's*, R. R. Boyer and H. W. Rosenberg, Eds. (The Metallurgical Society of AIME, Warrendale, Pennsylvania, 1984), p. 69.

26. J. D. Boyd, Trans. ASM **62**, 977 (1969).

27. R. W. Schutz and D. E. Thomas, in *Metals Handbook*, 9th ed., Vol. 13 (ASM, Metals Park, Ohio, 1987), p. 669.

28. D. E. Thomas and S. R. Seagle, in *Titanium Science and Technology: Proceedings of the Fifth International Conference on Titanium*, Munich, Germany, 1984, Vol. 4, G. Lütjering, U. Zwicker, and W. Bunk, Eds. (Deutsche Gesellschaft Für Metallkunde) p. 2533.

29. V. I. Sarrak, G. A. Filippov, and G. G. Kush, Phys. Met. Metall. **55**, 94 (1983).

Table 1
COMPOSITION OF TITANIUM ALLOYS*

Element	TI-10-2-3	TI-13-11-3	Beta-C	TI-6-4
Al	3.025	3.14	3.0	6.40
B	0.001	0.001		
C	0.017	0.010	0.01	0.016
Cr		11.41	6.0	
Cu	0.001	0.002		
Fe	1.945	0.12	0.06	0.16
Mn	0.004	0.006		
Mo	0.031	3.9	0.006	
N	0.008	0.013	0.018	0.009
O	0.097	0.097	0.093	0.19
Si	0.039	0.012		
Sn	0.010			
Ti	Bal.	Bal.	Bal.	Bal.
V	9.795	13.82	8.0	4.10
Zr	0.001	3.8		
H	1 ppm	0.0178	97 ppm	0.007
Other		Y < 0.005	Nb 0.10 Y <50 ppm	

* wt% unless indicated.

Table 2
VALUES OF k_a AND J FOR AGED TI-10V-2Fe-3Al

Test	η (V)	E_c (V/SCE)	k_a (s^{-1})	J (nmol cm^{-2} s^{-1})	Mean k_a
1	-0.45	-0.546	0.073	0.175	
	-0.50	-0.589	0.073	0.192	0.072 ± 0.001
	-0.55	-0.650	0.070	0.191	
2	-0.50	-0.609	0.043	0.133	
	-0.55	-0.666	0.049	0.161	0.048 ± 0.003
	-0.60	-0.726	0.052	0.198	
3	-0.45	-0.729	0.059	0.151	
	-0.50	-0.792	0.066	0.230	0.063 ± 0.003
4	-0.50	-0.740	0.065	0.377	
	-0.55	-0.814	0.068	0.481	0.067 ± 0.002
5	-0.45	-0.780	0.074	0.285	
	-0.50	-0.851	0.075	0.422	0.075 ± 0.001
6	-0.45	-0.764	0.080	0.295	
	-0.50	-0.839	0.081	0.428	0.081 ± 0.001

Table 3
VALUES OF k_a AND J FOR BETA-C TI

State	Test	η (V)	E_c (V/SCE)	k_a (s^{-1})	J (nmol cm^{-2} s^{-1})	Mean k_a
Unaged	7	-0.35	-0.455	0.036	0.095	
		-0.40	-0.503	0.032	0.103	
		-0.45	-0.553	9.028	0.109	0.032 ± 0.002
		-0.50	-0.607	0.032	0.133	
		-0.55	-0.660	0.033	0.159	
	8	-0.35	-0.479	0.030	0.083	
		-0.40	-0.521	0.029	0.100	
		-0.45	-0.570	0.031	0.121	0.030 ± 0.001
		-0.50	-0.620	0.032	0.146	
		-0.55	-0.672	0.030	0.169	
Aged	9	-0.40	-0.800	0.086	0.047	
		-0.45	-0.834	0.074	0.057	0.083 ± 0.011
		-0.55	-0.911	0.070	0.092	
		-0.60	-0.967	0.101	0.159	
	10	-0.45	-0.781	0.095	0.082	
		-0.50	-0.826	0.097	0.107	0.092 ± 0.006
		-0.55	-0.859	0.081	0.115	
		-0.60	-0.926	0.096	0.212	

Table 4
VALUES OF k_a AND J FOR TI-13V-11Cr-3Al

State	Test	η (V)	E_c (V/SCE)	k_a (s^{-1})	J (nmol cm^{-2} s^{-1})	Mean k_a
Unaged	11	-0.45	-0.479	0.072	0.048	
		-0.50	-0.523	0.064	0.051	0.069 ± 0.004
		-0.55	-0.574	0.072	0.067	
	12	-0.40	-0.428	0.066	0.033	
		-0.45	-0.473	0.043	0.046	0.068 ± 0.018
		-0.50	-0.524	0.094	0.086	
Aged	13	-0.45	-0.984	0.15	0.13	
		-0.50	-1.038	0.14	0.17	0.14 ± 0.01
		-0.55	-1.094	0.14	0.22	
	14	-0.50	-1.050	0.15	0.18	
		-0.55	-1.119	0.17	0.26	0.16 ± 0.01

Table 5
VALUES OF k_a AND J FOR TI-6AI-4V

Test	η (V)	E_c (V/SCE)	k_a (s⁻¹)	J (nmol cm⁻² s⁻¹)	Mean k_a
15	-0.60	-0.782	0.061	0.070	
	-0.65	-0.846	0.066	0.107	0.064 ± 0.002
16	-0.55	-0.624	0.068	0.078	
	-0.60	-0.674	0.056	0.078	0.062 ± 0.004
	-0.65	-0.731	0.064	0.095	
	-0.70	-0.799	0.060	0.116	

Table 6
TRAPPING CONSTANTS FOR TITANIUM ALLOYS

Alloy	State	Phase[a]	k_a (s⁻¹)	D_L/D_α	k (s⁻¹)
Single-Phase					
Ti Grade 2	Unaged (low H)[b]	α	0.028 ± 0.002	1	0.028
Beta-C Ti	Unaged	β	0.031 ± 0.002	≥1	≥0.031
Ti Grade 2	Unaged (high H)[b]	α	0.040 ± 0.004	1	0.040
Ti-13-11-3	Unaged	β	0.069 ± 0.011	≥1	≥0.069
Multi-Phase					
Ti-6-4	As-received	α_p-β	0.063 ± 0.005	≥1	≥0.063
Ti-10-2-3	Aged	β-α_s	0.066 ± 0.009	≥1	≥0.066
Beta-C Ti	Aged	β-α_s	0.088 ± 0.010	≥1	≥0.088
Ti-13-11-3	Aged	β-α_s	0.15 ± 0.01	≥1	≥0.150

[a] α_p = primary α phase; α_s = secondary α phase.
[b] When the charging potential reaches approximately -0.93 V, k_a increases from 0.028 to 0.040 s⁻¹ [7].
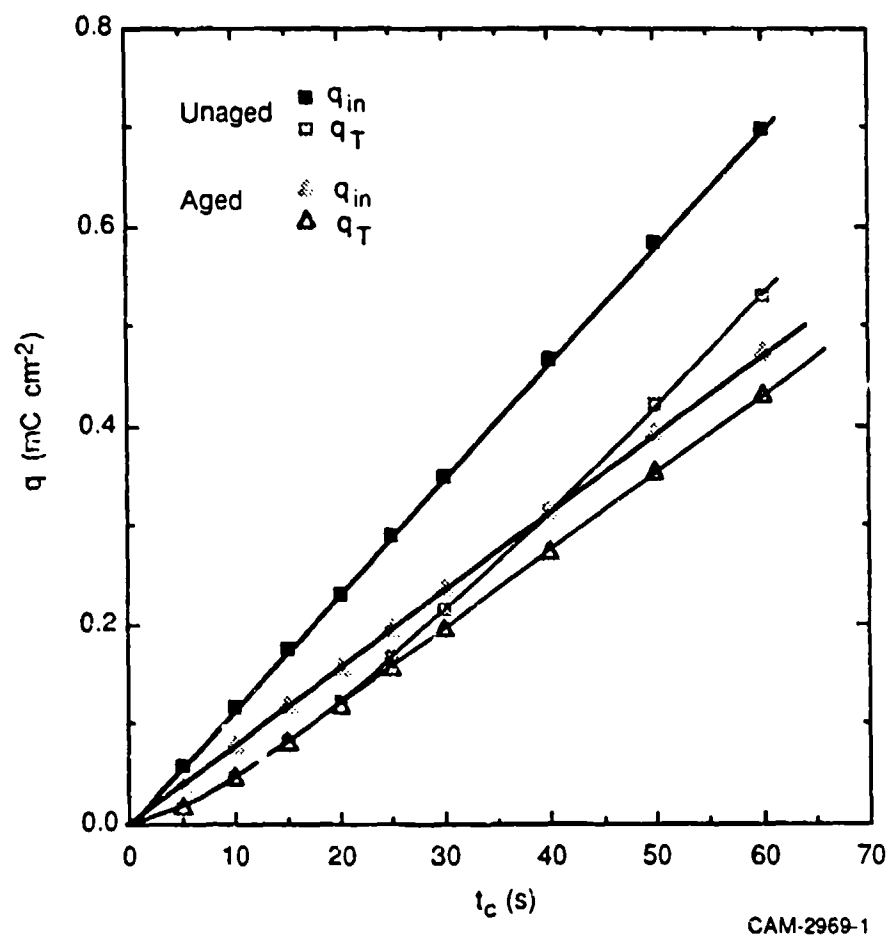
Figure 1. Dependence of q_{in} and q_T on charging time for Beta-C Ti. $\eta = -0.45$ V.
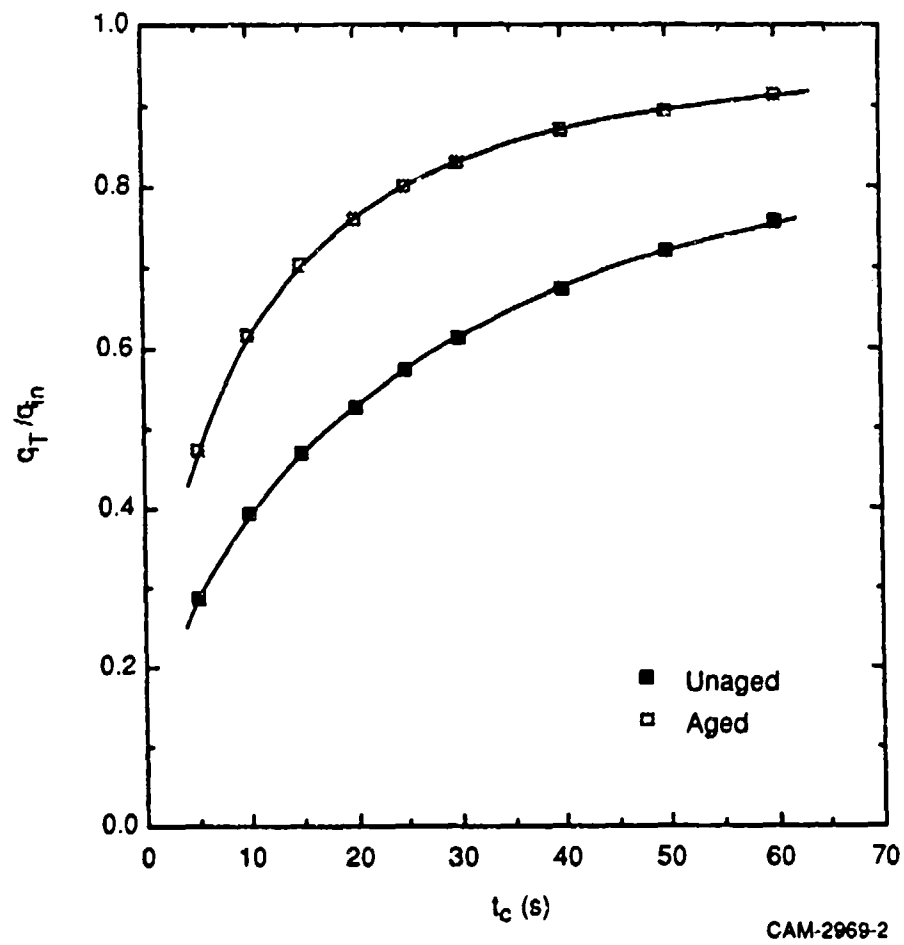
CAM-2969-1

Figure 2. Dependence of q_T/q_{in} on charging time for Beta-C Ti.

CAM-2969-3

Fig·ire 3. Dependence of q_a on charging time for Beta-C Ti.
$\eta = -0.45$ V.

1-19

q_a (mC cm^{-2})

0.08

0.06

0.04

0.02

0.00

1

2

3

□ Aged

■ Unaged

* Aged k_a ; Unaged J

0   10   20   30   40   50   60
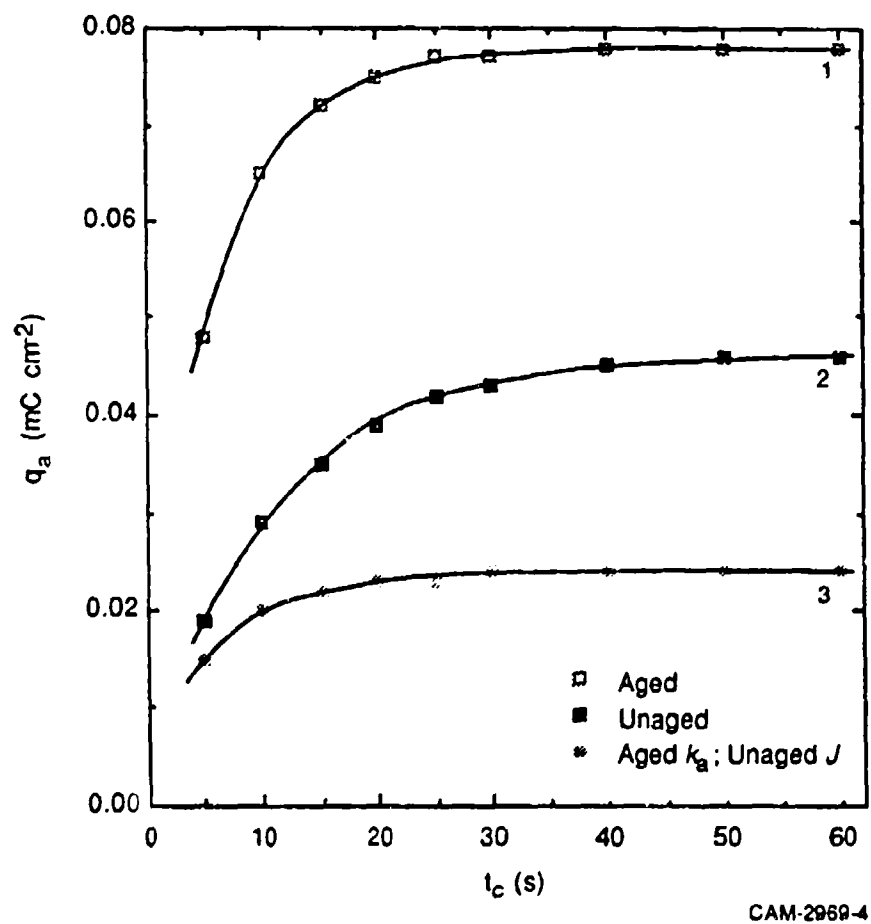
t_c (s)

CAM-2969-4
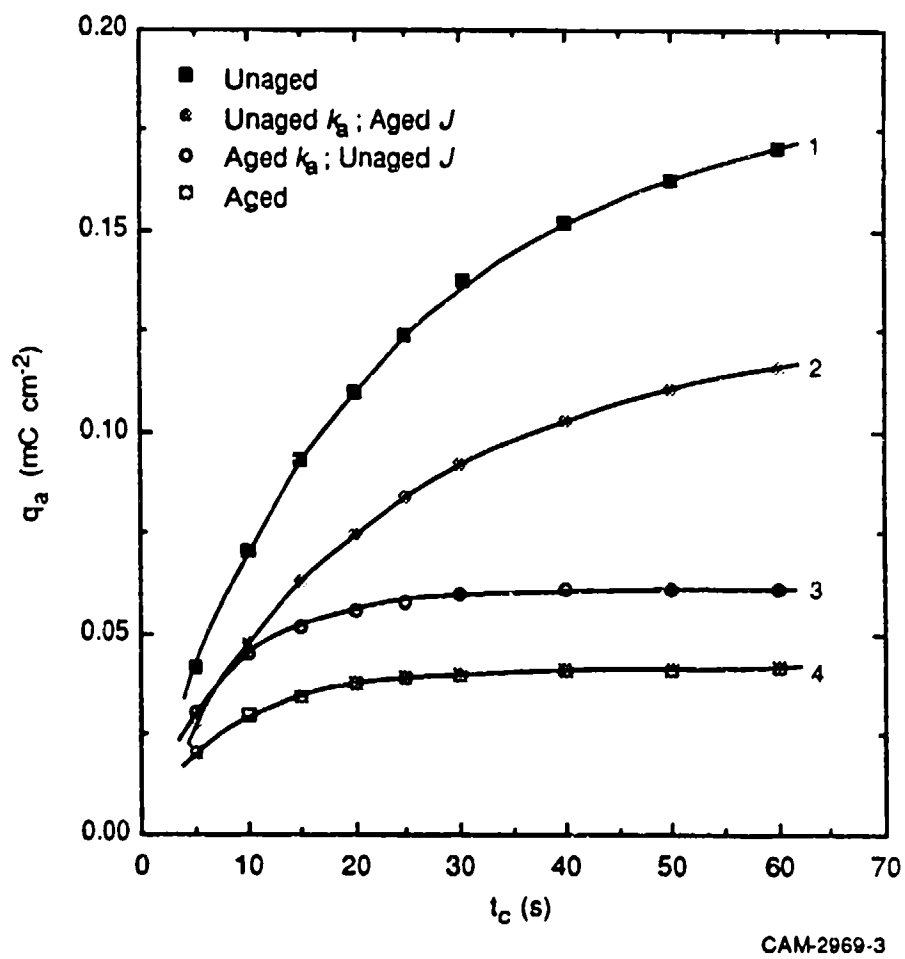
Figure 4. Dependence of q_a on charging time for Ti-13V-11Cr-3Al. η = -0.55 V.

1-20

HYDROGEN TRAPPING IN β-TITANIUM ALLOYS — THE LINK BETWEEN MICROSTRUCTURE AND HYDROGEN EMBRITTLEMENT

ABSTRACT

The ingress of hydrogen into two β-titanium alloys (Ti-15V-3Cr-3Al-3Sn and Beta-21S) was investigated so that the relationship between microstructure and hydrogen embrittlement (HE) could be examined in terms of trapping. Application of a technique referred to as hydrogen ingress analysis by potentiostatic pulsing (HIAPP) to the unaged and aged alloys in an acetate buffer (1 mol L^{-1} HAc/1 mol L^{-1} NaAc, where Ac = acetate) allowed the apparent trapping constant (k_a) and hydrogen entry flux to be evaluated in each case. Aging causes a negligible change in k_a for Ti-15-3, whereas a marked increase is observed for other β-Ti alloys; this increase matches the decrease in their tolerance to hydrogen. The trapping constant for aged Beta-21S is higher than that for aged Ti-15-3, reflecting the relative resistances to HE observed for these alloys. A comparison with other aged β-Ti alloys indicates that Ti-13-11-3 is the most susceptible to HE, followed by Beta-21S, Beta-C, Ti-10-2-3, and then Ti-15-3. The trapping constants for aged β-Ti alloys appear to be greatly affected by the α phase present at grain boundaries. The link between hydrogen trapping and location of the secondary α phase suggests that the resistance of aged β-Ti alloys to HE is primarily dependent on microstructure.

INTRODUCTION

Various β-titanium alloys are known to suffer a loss of ductility in hydrogen environments [1,2]. Aging enhances the susceptibility to hydrogen embrittlement (HE), as found for Beta-C Ti [3]. but it is often uncertain whether stress level or microstructure is primarily responsible for the differing suceptibilities of unaged and aged alloys or of different aged alloys. In a recent study [4], peak aged Beta-21S Ti was found to be susceptible to environmental cracking, which was presumed to involve HE, whereas peak aged Ti-15-3 appeared to be resistant. The higher susceptibility of Beta-21S was attributed to its higher yield strength and heavy α precipitation on β grain boundaries, although the relative influence of each factor was not established. Whatever the principal reason, it is evident that aged β-Ti alloys can differ considerably in their tolerance to hydrogen and this difference needs to be better understood.

The susceptibility of alloys to HE is strongly affected by hydrogen trapping at microstructural heterogeneities. The entry and trapping of hydrogen in various high-strength alloys have been investigated in previous work [5-8] using a technique referred to as hydrogen ingress analysis by potentiostatic pulsing (HIAPP), and it was established that the irreversible trapping capability can be correlated with the observed resistance to HE.

More recently, the use of HIAPP was extended to three ß-titanium alloys—Beta-C, Ti-10-2-3 (Ti-10V-2Fe-3Al), and Ti-13-11-3 (Ti-13V-11Cr-3Al) [9]. A marked increase in irreversible trapping was observed with aging and was attributed to precipitation of secondary α phase. During the present work, HIAPP was used to determine the trapping characteristics of two additional β-titanium alloys — Beta-21S and Ti-15-3. The objective was to explore the relationship between trapping and HE of these alloys and so determine whether the difference in their susceptibilities could be explained on the basis of microstructure.

EXPERIMENTAL PROCEDURE

Alloys

Specimens of Beta-21S (Ti-15Mo-2.7Nb-3Al-0.2Si-0.15O) and Ti-15-3 (Ti-15V-3Cr-3Al-3Sn) were obtained in both the solution treated and peak aged conditions [4]. The solution treatments that had been used for the Beta-21S and Ti-15-3 were 871°C for 8 h and 816°C for 30 min, respectively. Both alloys were peak aged at 538°C for 8 h. The yield strengths of the aged Beta-21S and Ti-15-3 were 1380 and 1315 MPa, respectively. Cylindrical sections 0.95 cm in diameter were machined from the specimens for use as electrodes. The alloys were examined in both the unaged and aged conditions to determine the effect of the secondary α phase on hydrogen ingress.

Technique

Details of the electrochemical cell and instrumentation have been given previously [5]. The test electrodes of each alloy consisted of the cylindrical sections (0.64-0.95 cm in length) press-fitted into a Teflon sheath so that only the planar end surface was exposed to the electrolyte. The surface was polished before each experiment with SiC paper followed by 0.05-μm alumina powder. The electrolyte was an acetate buffer (1 mol L^{-1} acetic acid/1 mol L^{-1} sodium acetate) containing 15 ppm As$_2$O$_3$ as a hydrogen entry promoter. The electrolyte was deaerated with argon for 1 h before measurements began and throughout data acquisition. The potentials were measured with respect to a saturated calomel electrode (SCE). All tests were performed at 22 ± 1°C.

The alloy of interest was subjected to a cathodic pulse E_c of duration t_c, after which the potential was maintained at a value 10 mV negative of the open-circuit potential E_{oc} [5,10,11]. Anodic current transients with a charge q_a were obtained over a range of charging times (5-60 s) at different overpotentials ($\eta = E_c - E_{oc}$). The open-circuit potential of the alloy was sampled immediately before each charging time and was also used to monitor the stability of the surface oxide.

ANALYSIS

Diffusion/Trapping Model

The anodic current transients were analyzed using a diffusion/trapping model [5,10] based on interface-limited diffusion control (referred to simply as interface control), whereby the rate of hydrogen ingress in an alloy is controlled by diffusion but the entry flux of hydrogen across the interface is restricted. According to this model, the total charge (C m^{-2}) passed out is given by

$$q'(\infty) = FJt_c\{1 - e^{-R}/(\pi R)^{1/2} - [1 - 1/(2R)]\text{erf}(R^{1/2})\} \tag{1}$$

where F is the Faraday constant, J is the ingress flux in mol m^{-2} s^{-1}, and $R = k_a t_c$. The charge $q'(\infty)$ is equated to q_a; the adsorbed charge is almost invariably found to be negligible, and so q_a can be associated entirely with absorbed hydrogen. k_a is an apparent trapping constant measured for irreversible traps in the presence of reversible traps and can be expressed by $k(D_a/D_L)$ where k is the irreversible trapping constant, D_a is the apparent diffusivity, and D_L is the lattice diffusivity of hydrogen in the metal.

In all cases except unaged Beta 21S (discussed below), Eq. (1) could be fitted to data for q_a to obtain values of k_a and J such that J was constant over the range of charging times and k_a was independent of charging potential, as is required for the model to be valid. Experimental and fitted values of q_a for aged Ti-15-3 are compared in Fig. 1, which illustrates the level of agreement obtained over the range of charging times for the alloys in this work.

The values of k_a and J can be used to calculate both the irreversibly trapped charge (q_T) given by

$$q_T = FJ(t_c/k_a)^{1/2}\{[R^{1/2} - 1/(2R^{1/2})]\text{erf}(R^{1/2}) + e^{-R}/\pi^{1/2}\} \tag{2}$$

and the hydrogen entry charge (q_{in}) from $q_{in} = FJt_c$, thereby allowing the trapping efficiency, q_T/q_{in}, to be obtained.

Ti-15V-3Cr-3Al-3Sn

Values of k_a and J for two tests on both the unaged and aged alloy are given in Table 1. In both cases, k_a was independent of charging potential. The overall mean values of k_a for the unaged and aged alloys were 0.042 ± 0.003 s^{-1} and 0.045 ± 0.005 s^{-1}, respectively, indicating that aging has little effect on the trapping characteristics of Ti-15-3. The flux increases with potential because of its dependence on the surface coverage of adsorbed hydrogen.

Beta-21S Ti

The anodic charge for unaged Beta-21S, like that for Ti-10-2-3 [9], generally did not increase with t_c, which implies that hydrogen entry does not occur to a significant degree. Hence, k_a could not be determined in this case.

Aged Beta-21S did exhibit a dependence of q_a on t_c, reflecting a rise in the rate of hydrogen entry compared with that for the unaged alloy. An increase in J with aging was also observed for Ti-10-2-3 and Ti-13-11-3 [9]. Notwithstanding the increase in J for aged Beta-21S, the change in q_a with charging time was small, with the result that the values of k_a and J were subject to considerable scatter. Values of k_a and J for two tests are shown in Table 2. Despite the scatter, k_a appears to be independent of charging potential. The mean value of k_a for the two tests is 0.099 ± 0.012 s^{-1}. As with Ti-15-3, the flux increases with potential.

Beta-21S has a higher trapping efficiency than Ti-15-3 (Fig. 2), reflecting its much higher value of k_a. The trapping efficiencies are high for both alloys, reaching 0.8 or higher at longer charging times. In the case of Beta-21S, q_T/q_{in} eventually exceeds 0.9, which indicates that as hydrogen accumulates in the metal, nearly all of it becomes trapped.

DISCUSSION

Irreversible Trapping Constants

Previous work [5-7], as noted above, showed that the irreversible trapping constants for steels and nickel-containing alloys can be correlated with the observed resistance to HE. The irreversible trapping constant (k) is calculated from k_a by using diffusivity data for the "pure" alloy to obtain the lattice diffusivity (D_L) and for the actual alloy to obtain the apparent diffusivity (D_a). The "pure" alloy is considered to be Ti with its principal alloying elements, so minor elements are assumed to be primarily responsible for reversible trapping in the actual alloys. The role of defects such as vacancies and edge dislocations in reversible trapping should also be considered, but the

diffusivities for β-Ti alloys appear to be low enough that reversible trapping at defects can be ignored [9].

Few data are available in the literature for the diffusivity of hydrogen in β-Ti alloys, with or without minor alloying elements, so it is difficult to evaluate k. However, the diffusivity for β-Ti alloys at 25°C is on the order of 10^{-11} m^2 s^{-1} [12], which is low enough that minor elements are unlikely to affect the diffusivity to a degree that is markedly different between the alloys. Accordingly, D_L/D_a is assumed to be similar for the different alloys in the unaged condition. Also, D_L should differ little between the unaged and aged conditions, as should D_a, since the α-phase precipitated during aging is considered to have little effect in terms of reversible trapping, as discussed previously [9]. Hence, D_L/D_a is considered to have the same value for both unaged and aged β-Ti alloys, thereby allowing the respective values of k_a — rather than k — to be compared in terms of the susceptibility to HE.

The mean values of the trapping constants for Ti-15-3 and aged Beta-21S are summarized in Table 3 along with those obtained previously for other β-Ti alloys as well as Ti-6Al-4V and titanium grade 2. If the minor elements in the β alloys are assumed to contribute only slightly to reversible trapping for diffusivities on the order of 10^{-11} m^2 s^{-1}, a lower limit can be obtained for k in each case, as given in Table 3, but it is of little value in assessing the relative susceptibility of different alloys.

Susceptibility to HE

Among the aged β-Ti alloys, Ti-13-11-3 has the highest value of k_a, followed by Beta-21S, Beta-C, Ti-10-2-3, and then Ti-15-3. The trapping constants for Beta-21S and Ti-15-3 are consistent with the relative resistances of these alloys to HE, as determined by Young and Gangloff [4]. Thus, the correlation between the resistance to HE and the trapping capability observed for steels and nickel-containing alloys appears to be applicable also to the β-Ti alloys. Ti-13-11-3 is therefore expected to be the least resistant on the basis of its trapping constants. At the other extreme, the low trapping constant for Ti-15-3 is consistent with the high resistance to HE reported for this alloy [4].

In the case of Ti-15-3, k_a and therefore k do not change significantly with aging, whereas they increase markedly for the other β-Ti alloys, paralleling the reported decrease in their tolerance to hydrogen [13]. The higher k_a and k were attributed [9] to irreversible trapping at the α/β interface and possibly in the α phase, presumably in addition to the irreversible trapping occurring at other sites that are also present in the unaged alloys.

Changes in k_a appear to be related to the presence of grain boundary α-phase. Aged Ti-15-3 contains a homogeneous distribution of fine α phase throughout each grain [4], whereas aged Ti-10-2-3, for example, has a continuous α layer precipitated at the β grain boundaries [14]. Thus, the negligible effect of aging on k_a in the case of Ti-15-3 is attributed to the lack of preferential α precipitation at grain boundaries, while the large increase in k_a for Ti-10-2-3 is consistent with the extensive α precipitation at grain boundaries.

The apparent relationship between hydrogen trapping and location of the secondary α phase suggests that the resistance of aged β-Ti alloys to HE is primarily dependent on microstructure. In particular, the high k_a for aged Beta-21S is commensurate with its observed susceptibility and reflects the microstructure of this alloy, which, unlike Ti-15-3, contains considerable grain boundary α phase as well as fine intragranular α platelets [4]. Thus, the resistance to HE, as indicated by k_a, appears to depend on the degree of α precipitation at grain boundaries rather than that within the grains. Further support for this dependence is provided by Beta-III Ti, which contains an almost continuous α layer at the grain boundaries and is susceptible to cracking [14].

SUMMARY

The ingress of hydrogen in two β-Ti alloys — Beta-21S and Ti-15-3 — shows marked differences that can be correlated with the ingress behavior in other β-Ti alloys.

- Aging causes a negligible change in k_a for Ti-15-3 but a marked increase for other β-Ti alloys, paralleling the decrease in their tolerance to hydrogen.

- The trapping constant for aged Beta-21S is higher than that for aged Ti-15-3, reflecting the relative resistances to HE observed for these alloys. A comparison with other aged β-Ti alloys indicates that Ti-13-11-3 is the most susceptible to HE, followed by Beta-21S, Beta-C, Ti-10-2-3, and then Ti-15-3. The low trapping constant for Ti-15-3 is consistent with its high resistance to HE.

- The magnitude of k_a for aged β-Ti alloys appears to be greatly affected by the degree of α precipitation at grain boundaries. The low value of k_a for Ti-15-3 reflects a lack of preferential α precipitation on grain boundaries, whereas the high k_a for aged Beta-21S is indicative of the considerable grain boundary α phase in that alloy.

- The apparent relationship between hydrogen trapping and location of the secondary α phase suggests that the resistance of aged β-Ti alloys to HE is primarily dependent on microstructure.

ACKNOWLEDGEMENTS

REFERENCES

1. N. E. Paton, R. A. Spurling, and C. G. Rhodes, in *Hydrogen Effects in Metals: Proceedings of the Third International Conference on the Effect of Hydrogen on Behavior of Materials*, Moran, Wyoming, 1980, I. M. Bernstein and A. W. Thompson, Eds. (The Metallurgical Society of AIME, Warrendale, Pennsylvania, 1981), p. 269.

2. P. A. Blanchard, R. J. Quigg, F. W. Schaller, E. A. Steigerwald, and A. R. Troiano, WADC Technical Report 59-172, Wright-Patterson Air Force Base, Ohio (April, 1959); cited in Ref. 15.

3. D. E. Thomas and S. R. Seagle, in *Titanium Science and Technology: Proceedings of the Fifth International Conference on Titanium*, Munich, Germany, 1984, Vol. 4, G. Lütjering, U. Zwicker, and W. Bunk, Eds. (Deutsche Gesellschaft Für Metallkunde) p. 2533.

4. L. M. Young and R. P. Gangloff, in *Proceedings 7th World Conference on Titanium*, S. H. Froes, Ed. (The Metallurgical Society of AIME, Warrendale, Pennsylvania, 1992)

5 B. G. Pound, Corrosion **45**, 18 (1989).

6. B. G. Pound, Acta Metall. **38**, 2373 (1990).

7. B. G. Pound, Acta Metall. **39**, 2099 (1991).

8 B. G. Pound, Corrosion **47**, 99 (1991).

9. B. G. Pound, Acta Metall., submitted for publication (1993).

10. R. McKibbin, D. A. Harrington, B. G. Pound, R. M. Sharp, and G. A. Wright, Acta Metall. **35**, 253 (1987).

11. B. G. Pound, R. M. Sharp, and G. A. Wright, Acta Metall. **35**, 263 (1987).

12. W. R. Holman, R. W. Crawford, and F. Paredes, Jr., Trans. Met. Soc. AIME **233**, 1836 (1965).

13. R. W. Schutz and D. E. Thomas, in *Metals Handbook*, 9th ed., Vol. 13 (ASM, Metals Park, Ohio, 1987), p. 669.

14. J. H. Giovanola, R. 'W. Klopp, J. W. Simons, T. Kobayashi, and D. A. Shockey, "Influence of Microstructure and M ·rodamage Processes on Fracture at High Loading Rates," SRI

International Final Report, Air Force Office of Scientific Research, Contract No. F49620-86-K-0010 (1989).

15. J. A. Feeney and M. J. Blackburn, Metall. Trans. 1, 3309 (1970).

Table 1
VALUES OF k_a AND J FOR TI-15-3

State	Test	η (V)	E_c (V/SCE)	k_a (s^{-1})	J (nmol cm^{-2} s^{-1})	Mean k_a
Unaged	1	-0.40	-0.472	0.043	0.110	
		-0.45	-0.520	0.047	0.135	
		-0.50	-0.573	0.038	0.134	0.043 ± 0.003
		-0.55	-0.632	0.045	0.161	
		-0.60	-0.696	0.040	0.167	
	2	-0.40	-0.472	0.040	0.107	
		-0.45	-0.519	0.033	0.111	
		-0.50	-0.571	0.042	0.140	0.042 ± 0.004
		-0.55	-0.626	0.049	0.169	
		-0.60	-0.686	0.045	0.178	
		-0.65	-0.750	0.043	0.195	
Aged	3	-0.45	-0.565	0.040	0.071	
		-0.50	-0.612	0.045	0.089	
		-0.55	-0.664	0.042	0.092	0.045 ± 0.004
		-0.60	-0.722	0.041	0.100	
		-0.65	-0.785	0.047	0.125	
		-0.70	-0.854	0.055	0.161	
	4	-0.50	-0.602	0.052	0.097	
		-0.55	-0.646	0.040	0.096	
		-0.60	-0.698	0.038	0.104	0.046 ± 0.006
		-0.65	-0.756	0.044	0.133	
		-0.70	-0.820	0.054	0.176	

Table 2
VALUES OF k_a AND J FOR AGED BETA-21S TI

Test	η (V)	E_c (V/SCE)	k_a (s^{-1})	J (nmol cm^{-2} s^{-1})	Mean k_a
5	-0.40	-0.742	0.112	0.048	
	-0.45	-0.782	0.080	0.049	0.096 ± 0.016
6	-0.55	-0.767	0.085	0.087	
	-0.60	-0.830	0.111	0.134	0.100 ± 0.010
	-0.65	-0.900	0.095	0.187	
	-0.70	-0.966	0.108	0.294	

Table 3
TRAPPING CONSTANTS FOR TITANIUM ALLOYS

Alloy	State	Phase[a]	k_a (s^{-1})	D_L/D_v	k (s^{-1})
Single-Phase					
Ti Grade 2	Unaged (low H)[b]	α	0.028 ± 0.002	1	0.028
Beta-C	Unaged	β	0.031 ± 0.002	≥1	≥0.031
Ti Grade 2	Unaged (high H)[b]	α	0.040 ± 0.004	1	0.040
Ti-15-3	Unaged	β	0.042 ± 0.003	≥1	≥0.042
Ti-13-11-3	Unaged	β	0.069 ± 0.011	≥1	≥0.069
Multi-Phase					
Ti-15-3	Aged	β-α_S	0.045 ± 0.005	≥1	≥0.045
Ti-6-4	As-received	α_p-β	0.063 ± 0.005	≥1	≥0.063
Ti-10-2-3	Aged	β-α_S	0.066 ± 0.009	≥1	≥0.066
Beta-C	Aged	β-α_S	0.088 ± 0.010	≥1	≥0.088
Beta-21S	Aged	β-α_S	0.099 ± 0.012	≥1	≥0.099
Ti-13-11-3	Aged	β-α_S	0.15 ± 0.01	≥1	≥0.150

[a] α_p = primary α phase; α_S = secondary α phase.

[b] When the charging potential reaches approximately -0.93 V, k_a increases from 0.028 to 0.040 s^{-1} [8].
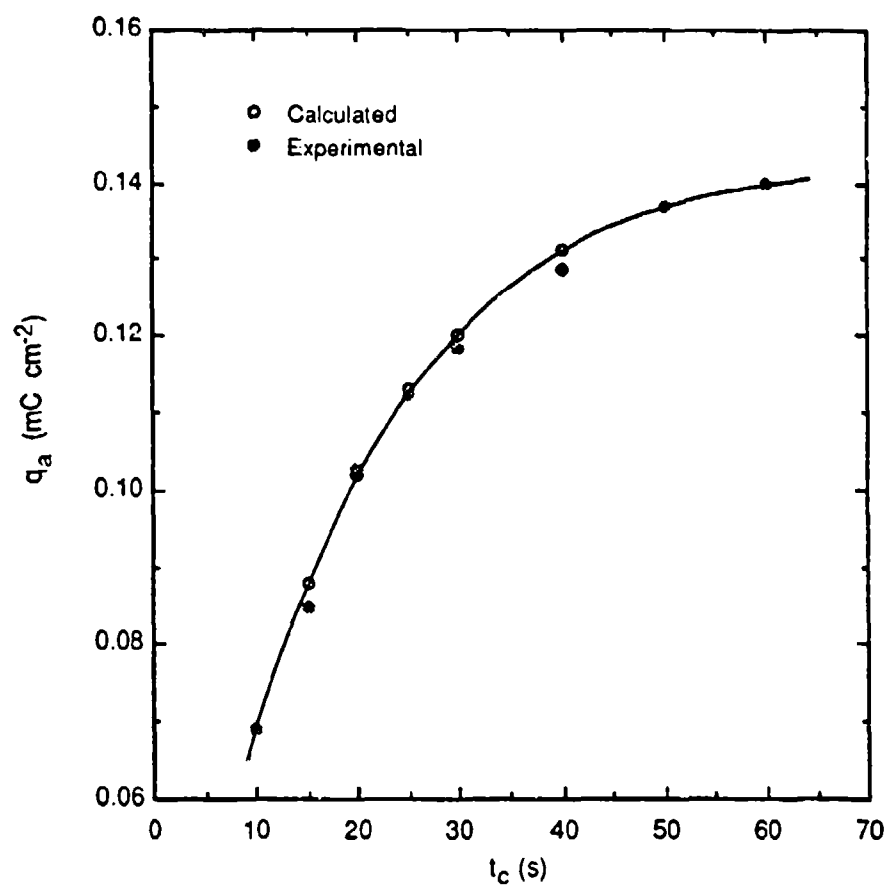
Figure 1. Dependence of q_a on charging time for aged Ti-15-3.
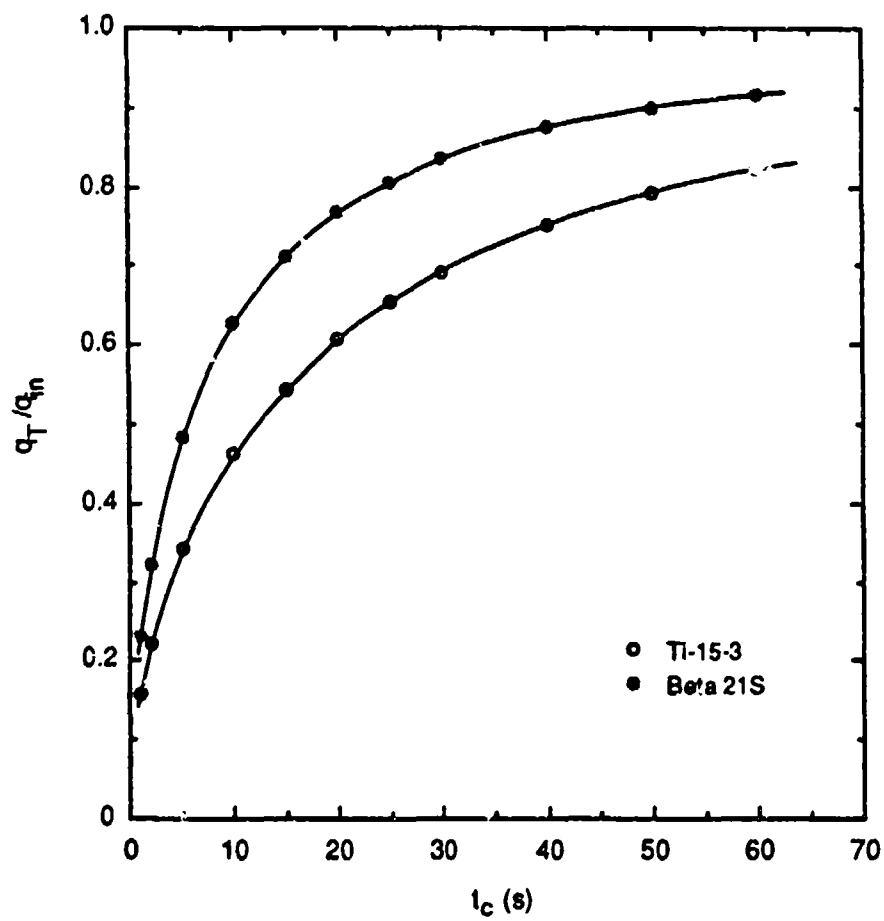$\eta = -0.45$ V; $k_a = 0.044$ s^{-1}, $J = 0.133$ nmol cm^{-2} s^{-1}.

Figure 2. Dependence of q_T/q_{in} on charging time for aged Beta-21S and Ti-15-3.

THE INGRESS OF HYDROGEN INTO COPPER-NICKEL ALLOYS

ABSTRACT

The ingress of hydrogen into two copper-nickel alloys — Marinel (aged) and Monel K-500 (unaged and aged) — was studied using a technique referred to as hydrogen ingress analysis by potentiostatic pulsing (HIAPP). Anodic current transients obtained for these alloys in an acetate buffer (1 mol L^{-1} HAc/1 mol L^{-1} NaAc, where Ac = acetate) were analyzed using a diffusion/ trapping model to determine the trapping constants and hydrogen entry fluxes. A small increase was observed in the irreversible trapping constant for alloy K-500 with aging. The trapping constants of the aged alloys are similar within the limits of uncertainty, but the hydrogen entry flux for Marinel is lower than that for either aged or unaged alloy K-500. The lower flux could account, at least partly, for the higher resistance to hydrogen embrittlement reported for Marinel. The trap densities are qualitatively consistent with the levels of sulfur and phosphorus in the two alloys, which supports the assumption that these species provide the primary irreversible traps.

INTRODUCTION

The susceptibility of alloys to hydrogen embrittlement (HE) is strongly influenced by the presence of microstructural heterogeneities, which can provide sites to trap hydrogen. The accumulation of hydrogen at second-phase particles and precipitates, for example, is considered to induce particle fracture or weakening of particle-matrix interfaces, thereby promoting the formation of microvoids. Incoherent precipitates tend to be particularly conducive to HE because they typically provide strong traps (high binding energy for hydrogen) with large saturabilities.[1-3]

For most alloys, the degradation that hydrogen causes in mechanical properties reflects the alloy's intrinsic susceptibility determined by the trapping characteristics.[4,5] However, the amount of hydrogen entering the alloy can play a critical role in determining whether embrittlement will actually occur. In some cases, an alloy may prove to be resistant during exposure because the amount of hydrogen that enters is not enough to allow some critical concentration to be exceeded at the traps. Likewise, if alloys have a similar intrinsic susceptibility in terms of trapping characteristics, the difference in their actual resistance to HE is then likely to be determined by the amount of hydrogen absorbed by each alloy. Consequently, alloys should be characterized in

terms of both trapping capability and rate of hydrogen entry to assess their likelihood of embrittlement.

An electrochemical technique referred to as hydrogen ingress analysis by potentiostatic pulsing (HIAPP) has been used in recent work to investigate the entry and trapping of hydrogen in a range of alloys.[4-8] In this technique, the alloy of interest is charged with hydrogen at a constant potential E_c for a time t_c. The potential is then stepped in the positive direction to a value 10 mV negative of the open-circuit potential E_{oc}. By using an appropriate diffusion/trapping model[6,9] to analyze the resulting anodic current transient, entry and trapping parameters have been determined for the various alloys studied to date. It was shown that a range of microstructural features can be identified as the principal irreversible traps and that the irreversible trapping constants for the alloys studied can be correlated with their observed resistances to HE. The pulse work also indicated that a knowledge of both the trapping capability and hydrogen entry rates can be used with some alloys to further account for differences found in their resistance to embrittlement.[6]

The present study involved the application of HIAPP to Marinel, a recently developed copper-nickel alloy, and Monel K-500, a 65 Ni-30 Cu alloy that had been examined previously[6,7] and was included here because its hydrogen ingress characteristics provided a useful comparison with those of Marinel, which contains 77 Cu-15 Ni. Although the Monel had been examined in previous work, subsequent refinements to both the pulse technique and the analysis made redetermination of its hydrogen ingress parameters worthwhile. The objective of this study was to investigate the hydrogen ingress behavior of these two alloys and so provide a basis for assessing their susceptibility to HE.

EXPERIMENTAL PROCEDURE

The composition of each alloy was provided by the producer and is given in Table 1. The Marinel was supplied as rod with a diameter of 2.4 cm. The as-received alloy had been aged to a yield strength of 793 MPa and was not treated further. The Monel K-500 was received as unaged, 1.27-cm-diameter, cold-drawn rod with a yield strength of about 758 MPa. A section of the rod was age-hardened to give a yield strength of about 1096 MPa. During aging, particles of Ni_3 (Ti,Al) are precipitated throughout the matrix of alloy K-500,[10] whereas the particles in Marinel are believed to be Ni_3Al and Ni_3Nb.[11]

Details of the electrochemical cell and instrumentation have been given previously.[6] The test electrodes of each alloy consisted of a 3.8-cm length of rod (1.27 cm in diameter) press-fitted into a polytetrafluoroethylene sheath so that only the planar end surface was exposed to the electrolyte. The surface was polished before each experiment with SiC paper followed by 0.05-

μm alumina powder. The electrolyte contained 1 mol L^{-1} acetic acid and 1 mol L^{-1} sodium acetate with 15 ppm As_2O_3 and was deaerated continuously with argon before and throughout data acquisition. The potentials were measured with respect to a saturated calomel electrode (SCE). All tests were performed at $22 \pm 1°C$.

The test electrode was charged with hydrogen for times from 5 s to 60 s for each E_c. Anodic current transients with a charge q_a were obtained for each charging time over a range of cathodic overpotentials ($\eta = E_c - E_{oc}$). The open-circuit potential of the test electrode was sampled immediately before each pulse.

RESULTS

Analysis

The current transients were analyzed using a diffusion/trapping model[6,9] in which the rate of hydrogen ingress is controlled by diffusion but the entry flux across the interface is restricted. According to the model, the total anodic charge (C m^{-2}) passed out is given by

$$q'(\infty) = FJt_c\{1 - e^{-R}/(\pi R)^{1/2} - [1 - 1/(2R)]erf(R^{1/2})\} \qquad (1)$$

where F is the Faraday constant, J is the ingress flux in mol m^{-2} s^{-1}, and $R = k_a t_c$. The charge $q'(\infty)$ is equated to q_a, which can be associated entirely with absorbed hydrogen because the adsorbed charge is invariably found to be negligible. k_a is an apparent trapping constant measured for irreversible traps in the presence of reversible traps and is related to the rate constant for irreversible trapping (k) by $k(D_a/D_L)$, where D_a is the apparent diffusivity and D_L is the lattice diffusivity of hydrogen in the metal.

For the model to be applicable, it must be possible to determine a trapping constant for which the ingress flux is independent of charging time over the range of interest. It was found that data for q_a could be fitted to Equation (1) to obtain values of k_a and J that satisfied this requirement at each potential. These values were then used to calculate the irreversibly trapped charge (q_T) given by

$$q_T = FJ(t_c/k_a)^{1/2}\{[R^{1/2} - 1/(2R^{1/2})]erf(R^{1/2}) + e^{-R}/\pi^{1/2}\} \qquad (2)$$

The charge associated with the entry of hydrogen into the metal (q_{in}) can be determined from $q_{in} = FJt_c$, and so the trapping efficiency, q_T/q_{in}, can be evaluated.

The density of particles or defects (N_i) providing irreversible traps can be obtained from the apparent trapping constant by using a model[4,12] based on spherical traps:

$$N_i = k_a a/(4\pi d^2 D_a) \tag{3}$$

where a is the diameter of the metal atom and d is the trap radius, which is estimated from the dimensions of heterogeneities that are potential irreversible traps. The value of a for an alloy is taken as the mean of the atomic diameters weighted in accordance with the atomic fraction of each element. Trap densities are calculated for appropriate values of d, so that the dominant irreversible trap can be identified by comparing the values of N_i with the actual concentrations of specific heterogeneities in the alloy.

Marinel

Values of k_a and J for two tests on Marinel are given in Table 2. In both cases, k_a is independent of charging potential, as is required for the model to be valid, since the trapping characteristics should be unaffected by electrochemical conditions at the metal surface. The overall mean value of k_a was 0.034 ± 0.004 s^{-1}.

The flux was constant over the range of charging times for each overpotential and, as expected, increased with overpotential because of the dependence of J on the surface coverage of adsorbed hydrogen. The surface coverage is assumed to respond rapidly to changes in potential, so the flux should exhibit an exponential dependence on potential. Log J is indeed observed to vary linearly with η (Figure 1), indicating that the coverage response is very fast.

Monel K-500

Values of k_a and J for tests on both the unaged and aged alloy are given in Table 3. As with Marinel, k_a was independent of charging potential. The overall mean values of k_a for the unaged and aged alloys were 0.017 ± 0.003 s^{-1} and 0.021 ± 0.003 s^{-1}, respectively. Again, the flux generally increased with overpotential (Figure 1).

The trapping constant for the aged alloy is in agreement with the average value (0.021 s^{-1}) obtained for a range of electrolytes in the earlier work.[7] Although a difference in trapping behavior between unaged and aged alloy K-500 was not apparent previously, improvements in data acquisition now reveal that the trapping constant of the aged alloy is a little higher than that of the unaged alloy.

Trapping Efficiencies

The trapping efficiencies for the Marinel and alloy K-500 are shown in Figure 2. Clearly, Marinel has the highest trapping efficiency for a given charging time, followed by aged and unaged alloy K-500, reflecting the order of their apparent trapping constants. The higher k_a for the Marinel not only results in a higher value of q_T/q_{in} for each charging time but also enhances the increase in trapping efficiency with charging time up to $t_c = 30$ s. The flux has no effect on the trapping efficiency, since both q_{in} and q_T have the same dependence on J.

DISCUSSION

Irreversible Trapping Constants

The mean values of the trapping constants for the two alloys are given in Table 4. Evaluation of k from k_a requires diffusivity data for the pure Ni-Cu alloy to obtain D_L and for the actual alloy to obtain D_a, so that the effect of reversible traps can be taken into account. As in our previous work[4-7] on nickel-base alloys, the minor alloying elements are assumed to be primarily responsible for the reversible trapping behavior in Marinel and alloy K-500. Defects such as vacancies or edge dislocations are not expected to contribute significantly to reversible trapping because the binding energy of hydrogen to such defects in an fcc lattice is a factor of 4 smaller than the activation energy for diffusion.[13]

Alloy K-500. The lattice diffusivity was determined by interpolation of data for a range of binary Cu-Ni alloys and was found to be $(3.0 \pm 0.1) \times 10^{-14}$ m^2 s^{-1} for 35 wt% Cu-65% Ni at 25°C.[14] The level of Cu differs a little between the 35 Cu-65 Ni alloy and alloy K-500 (30% Cu), but the error in using the diffusivity of the 35 Cu alloy for D_L is considered to be negligible. The diffusivity for cold-worked and aged alloy K-500 (assumed to be at ambient temperature) is reported[15] to be 1.48×10^{-14} m^2 s^{-1}. By using these data for D_L and D_a, the value of k for the aged alloy is found to be 0.042 ± 0.007 s^{-1}.

No data were available for the diffusivity in the unaged alloy. Therefore, since D_a for the *aged* alloy is only about a factor of 2 smaller than D_L, it was assumed that the intermetallic particles precipitated during aging[10] have little effect on D_a compared with that of the minor alloying elements in solid solution. On this basis, the value of k for the unaged alloy is 0.034 ± 0.007 s^{-1}.

Marinel. The diffusivity of hydrogen in Marinel has been measured[16] as a function of temperature from about 270° to 700°C. Extrapolation to 25°C gives a value of approximately $(1 \pm 0.2) \times 10^{-14}$ m^2 s^{-1}. The lattice diffusivity was again evaluated using the data for Cu-Ni alloys and was estimated to be $(8 \pm 1) \times 10^{-15}$ m^2 s^{-1} for 15 wt% Ni-85% Cu at 25°C.[14] As with alloy K-

500, the level of Cu is lower in Marinel (76.8% Cu), but any effect on D_L can be ignored because of the uncertainties associated with obtaining D_L by interpolation and D_a by extrapolation. Clearly, the values of D_a and D_L do not differ significantly, the implication being that reversible traps have relatively little effect in Marinel. Since $D_L/D_a \approx 1$, k is taken as being equal to k_a and so has a value of 0.034 ± 0.015 s^{-1}.

Comparison of Ingress Characteristics

The apparent trapping constant for Marinel (aged) is higher than that for alloy K-500 (unaged and aged), but the more meaningful parameter in terms of HE is k.[4,5] Aged alloy K-500 has the highest value of k, followed by unaged alloy K-500 and Marinel together. Hence, aged alloy K-500 could be predicted to be more susceptible to HE than either the unaged alloy or Marinel. However, the uncertainty in the values of k renders them close enough that any difference in susceptibility of the aged alloys cannot be distinguished.

Interestingly, if the uncertainty in k is ignored, the order of the trapping constants is found to parallel that of the yield strengths of the unaged and aged alloy K-500 (758 and 1096 MPa, respectively) and the Marinel (793 MPa), which suggests that these alloys may follow the "rule of thumb" that susceptibility to HE is directly related to strength level. However, as pointed out by Thompson and Bernstein,[17] this "rule" can be a gross oversimplification, so conformance to it is not necessarily to be expected.

A marked difference between the two alloys is that Marinel has a smaller hydrogen entry flux, particularly compared with aged alloy K-500 for which the flux is typically 2-3 times larger at high overpotentials (Figure 1). The implication is that Marinel should be more resistant to embrittlement, if not because of a smaller trapping capability, then because of a slower buildup in the local concentration of hydrogen to some critical level required to initiate cracking. The effect of the difference in flux is illustrated in Figure 3, which compares the amount of irreversibly trapped hydrogen, as represented by q_T [Equation (2)], for Marinel and aged alloy K-500. At a given charging time, q_T is smaller for Marinel, showing that the lower flux more than compensates for the higher value of the apparent trapping constant.

Slow strain rate tests[18] have been performed on Marinel and alloy K-500 precharged and subsequently maintained at -1.0 V (SCE) in 3.5% NaCl. The pH of this solution was presumably 6-7, so the charging environment is roughly comparable to that provided by the weakly acidic acetate buffer (pH~5) used in the pulse tests. Both alloys appear to have been tested in the aged condition and, unlike the present specimens, were similar in strength. (Alloy K-500 rod in the cold drawn and aged condition can range in maximum yield strength, typically from 655 to 1103

MPa, depending on the size of the rod.[10]) Alloy K-500 was found to undergo a marked decrease in elongation and reduction of area, whereas Marinel exhibited little change after exposure for approximately twice as long. From the pulse tests, it appears that the difference in behavior is unlikely to be clearly attributable to irreversible trapping, particularly since the two specimens in the strain tests were similar in strength. However, from the results with the acetate buffer, the hydrogen entry flux for Marinel in 3.5% NaCl should likewise be significantly lower than that for either the unaged or aged alloy K-500. Therefore, since the intrinsic susceptibility of the aged alloys is similar within the uncertainty of k, the lower entry flux for Marinel must account, at least partly, for the higher resistance of this alloy to HE.

Identification of Traps

Alloy K-500. HE in Ni-Cu base alloys is known to be assisted by sulfur segregated at grain boundaries.[19] Since hydrogen also probably segregates to the grain boundaries as in nickel,[20] grain boundary sulfur was assumed to provide the irreversible traps predominantly encountered by hydrogen in alloy K-500. The density of irreversible traps (N_i) associated with atomic sulfur was calculated from the apparent trapping constants for the unaged and aged alloy by means of Equation (3). By using $D_a = 1.48 \times 10^{-14}$ m^2 s^{-1}, $d = 104 \times 10^{-12}$ m, and $a = 254 \times 10^{-12}$ m, N_i was found to be $(2.1 \pm 0.4) \times 10^{21}$ m^{-3} for the unaged alloy and $(2.7 \pm 0.4) \times 10^{21}$ m^{-3} for the aged alloy.

For comparison, the actual sulfur content (0.001 wt%) in the alloy corresponded to a concentration of 1.6×10^{24} atoms m^{-3}, which clearly indicates that the primary irreversible traps are not associated with *matrix* sulfur. The possibility that the traps do not involve sulfur at all cannot be discounted, as noted previously.[6] The other candidates most likely to provide the principal traps are TiN particles, which are generally present in alloy K-500.[10] However, the trap density of 1.3×10^{14} m^{-3} calculated in this case was about two orders of magnitude less than the concentration of TiN particles (1×10^{16} m^{-3}) in the present specimens, so these particles are ruled out as the primary traps. Moreover, since grain boundary sulfur is known to be implicated in HE of Ni-Cu alloys, it must be considered likely to act as the *principal* irreversible trap.

In principle, the role of segregated sulfur as the principal trap can be tested like that of the nitride particles, by comparing N_i with the grain boundary concentration of sulfur. The approach of matching N_i with the actual defect concentration has been successful in identifying irreversible traps such as carbide particles in nickel-base alloys.[4,5] However, it is more difficult in the case of grain boundary segregants, because segregation data are frequently lacking. Such data are available for Hastelloy C-276 (UNS N10276)[21] and previous work[5] has shown that it is possible for the trap density to be in close agreement with the amount of grain boundary phosphorus

distributed per unit volume of this alloy. Unfortunately, suitable data are unavailable for sulfur segregation in alloy K-500, but the results for alloy C-276 lend some support to the case for considering grain boundary sulfur as the primary irreversible trap in alloy K-500. Although actual verification in terms of calculated trap densities will not be possible until segregation data become available, further support is provided by a comparison of N_i values for alloy K-500 and Marinel with their relative metalloid levels, as discussed below.

Marinel. Since sulfur is known to segregate to grain boundaries in Ni[22] and Ni-Cu alloys,[19] and since Marinel, like alloy K-500, is a Cu-Ni alloy, it is reasonable to expect that segregation also occurs in this alloy and furthermore that its irreversible traps are probably associated with grain boundary sulfur and, in this case, phosphorus. The size (d) of the trap was taken as the mean atomic radius of sulfur and phosphorus weighted in accordance with their atomic fraction in the alloy. Therefore, with $k_a = 0.034$ s^{-1}, $d = 108 \times 10^{-12}$ m, $a = 257 \times 10^{-12}$ m, and $D_a = (1.0 \pm 0.2) \times 10^{-14}$ m^2 s^{-1}, the density of irreversible traps was calculated to be $(6.0 \pm 1.9) \times 10^{21}$ m^{-3}.

Even allowing for some difference in the degree of segregation, the trap density for Marinel is significantly higher than that for alloy K-500 and so is qualitatively consistent with the higher sulfur and phosphorus content of this alloy. Thus, a correlation appears to exist between the trap density and the levels of sulfur and phosphorus in these two copper-nickel alloys, which supports the assumption that these species provide the primary irreversible traps.

SUMMARY

- The ingress of hydrogen in two copper-nickel alloys (Marinel and alloy K-500) was shown to fit a diffusion/trapping model in which the hydrogen entry flux across the interface is restricted.

- Aged alloy K-500 has the highest value of k, and so it could be predicted to be more susceptible to HE than either the unaged alloy or as-received Marinel. However, the uncertainty in the values of k renders them close enough that any difference in susceptibility of the aged alloys cannot be distinguished.

- The entry flux for Marinel is smaller than that for alloy K-500, so the local concentration of hydrogen in Marinel should build up more slowly to some critical level. Since the difference in HE behavior of Marinel and alloy K-500 having similar strength does not appear to be clearly attributable to irreversible trapping, the lower entry flux for Marinel must account, at least partly, for the higher resistance to HE observed for this alloy.

- The primary irreversible traps are believed to involve sulfur and phosphorus segregated at grain boundaries, but a lack of data for grain boundary concentrations precludes verification in terms of calculated trap densities. Nevertheless, the trap densities for Marinel and alloy K-500 can be correlated with their sulfur and phosphorus levels, which supports the assumption that these species provide the primary irreversible traps.

ACKNOWLEDGEMENTS

REFERENCES

1 G. M. Pressouyre and I. M. Bernstein, Metall. Trans. **9A**, 1571 (1978).

2. G. M. Pressouyre and I. M. Bernstein, Acta Metall. **27**, 89 (1979).

3. R. Gibala and D. S. DeMiglio, in *Proceedings of the Third International Conference on Effect of Hydrogen on the Behavior of Materials*, I. M. Bernstein and A. W. Thompson, Eds. (The Metall. Soc. AIME, Moran, Wyoming, 1980), p. 113.

4 B. G. Pound, Acta Metall. **38**, 2373 (1990).

5. B. G. Pound, Acta Metall. **39**, 2099 (1991).

6. B. G. Pound, Corrosion **45**, 18 (1989).

7. B. G. Pound, Corrosion **46**, 50 (1990).

8. B. G. Pound, Corrosion **47**, 99 (1991).

9. R. McKibbin, D. A. Harrington, B. G. Pound, R. M. Sharp, and G. A. Wright, Acta Metall. **35**, 253 (1987).

10. *Monel Nickel-Copper Alloys*, 4th ed., Huntington Alloys (Huntington, West Virginia, 1981), p. 31.

11. C.D.S. Tuck, Personal communication, Langley Alloys Ltd (Berkshire, England, 1993).

12. B. G. Pound, R. M. Sharp, and G. A. Wright, Acta Metall. **35**, 263 (1987).

13. W. D. Wilson and S. C. Keeton, in *Advanced Techniques for Characterizing Hydrogen in Metals*, N. F. Fiore and B. J. Berkowitz, Eds. (The Metallurgical Society of AIME, Warrendale, Pennsylvania, 1981), p. 3.

14. H. Hagi, Trans. Jpn. Inst. Metals **27**, 233 (1986).

15. J. A. Harris, R. C. Scarberry, and C. D. Stephens, Corrosion **28**, 57 (1972).

16. C. D. S. Tuck, Z. Xianhua, and D. J. Talbot, Br. Corr. J., submitted for publication.

17. A. W. Thompson and I. M. Bernstein, in *Metallurgical Treatises*, J. K. Tien and J. Elliott, Eds. (The Metallurgical Society of AIME, Warrendale, Pennsylvania, 1981) p. 589.

18. R. Butler, paper presented at Conference on Marine Engineering with Copper Nickel, London, England (1988); cited in *Hiduron Marinel Alloy*, Technical Data Sheet, Langley Alloys, Ltd. (Berkshire, England, 1991).

19. J. D. Frandsen and H. L. Marcus, in *Effect of Hydrogen on Behavior of Materials*, A. W. Thompson and I. M. Bernstein, Eds. (The Metallurgical Society of AIME, Warrendale, Pennsylvania, 1976), p. 233.

20. D. H. Lassila and H. K. Birnbaum, Acta Metall. **35**, 1815 (1987).

21. B. J. Berkowitz and R. D. Kane, Corrosion **36**, 24 (1980).

22. S. M. Bruemmer, R. H. Jones, M. T. Thomas, and D. R. Baer, Metall. Trans. **14A**, 223 (1983).

Table 1
COMPOSITION (wt%) OF COPPER-NICKEL ALLOYS

Element	Marinel	Alloy K-500
Al	1.61	2.92
C	0.010	0.16
Cr	0.40	-
Cu	76.8	29.99
Fe	0.96	0.64
Mg	0.02	-
Mn	4.36	0.72
Nb	0.69	-
Ni	15.00	64.96
P	0.010	-
Pb	0.007	-
S	0.005	0.001
Si	0.05	0.15
Sn	<0.02	-
Ti	-	0.46
Zn	0.02	-

Table 2
VALUES OF k_a AND J FOR MARINEL

Test	η (V)	E_c (V/SCE)	k_a (s^{-1})	J (nmol cm^{-2} s^{-1})	Mean k_a
1	-0.25	-0.355	0.027	0.045	
	-0.30	-0.407	0.040	0.049	
	-0.35	-0.460	0.037	0.054	
	-0.40	-0.512	0.036	0.056	0.034 ± 0.004
	-0.55	-0.665	0.032	0.059	
	-0.60	-0.710	0.031	0.070	
2	-0.25	-0.374	0.034	0.038	
	-0.35	-0.471	0.037	0.040	
	-0.40	-0.524	0.029	0.036	
	-0.45	-0.577	0.039	0.043	0.035 ± 0.003
	-0.50	-0.630	0.036	0.045	
	-0.55	-0.678	0.032	0.057	

Table 3
VALUES OF k_a AND J FOR ALLOY K-500

State	Test	η (V)	E_c (V/SCE)	k_a (s^{-1})	J (nmol cm^{-2} s^{-1})	Mean k_a
Unaged	3	-0.30	-0.386	0.014	0.095	
		-0.35	-0.442	0.025	0.137	
		-0.40	-0.495	0.021	0.133	
		-0.45	-0.548	0.017	0.128	0.018 ± 0.003
		-0.50	-0.602	0.016	0.143	
		-0.55	-0.660	0.017	0.164	
	4	-0.25	-0.333	0.015	0.058	
		-0.30	-0.384	0.017	0.070	
		-0.35	-0.439	0.014	0.071	0.015 ± 0.001
		-0.40	-0.492	0.013	0.082	
Aged	5	-0.25	-0.344	0.023	0.046	
		-0.30	-0.388	0.015	0.062	
		-0.35	-0.432	0.022	0.107	0.020 ± 0.003
		-0.40	-0.480	0.022	0.137	
		-0.45	-0.528	0.018	0.153	
	6	-0.25	-0.319	0.018	0.083	
		-0.30	-0.372	0.026	0.184	
		-0.35	-0.423	0.024	0.201	0.022 ± 0.003
		-0.45	-0.526	0.022	0.199	
		-0.50	-0.578	0.019	0.202	
	7	-0.25	-0.310	0.018	0.100	
		-0.30	-0.366	0.022	0.146	
		-0.35	-0.417	0.022	0.176	0.020 ± 0.002
		-0.40	-0.468	0.021	0.192	
		-0.45	-0.520	0.017	0.184	

Table 4
TRAPPING CONSTANTS FOR COPPER-NICKEL ALLOYS

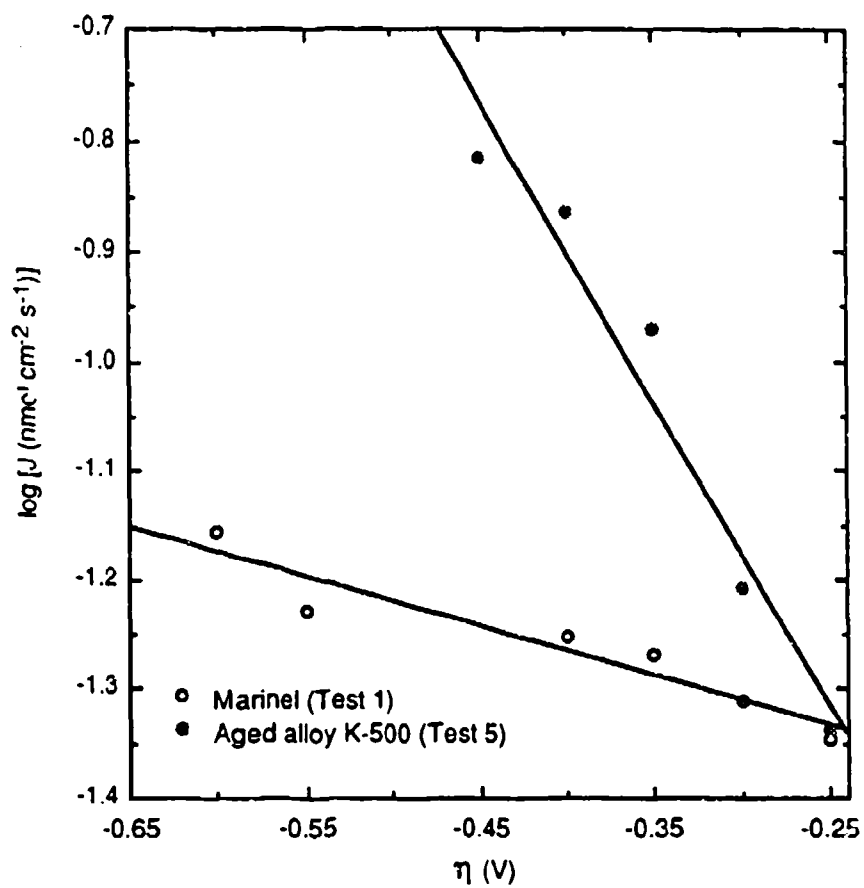| Alloy	State	k_a (s^{-1})	D_L/D_a	k (s^{-1})
Marinel	Aged	0.034 ± 0.004	~1	0.034 ± 0.015
K-500	Unaged	0.017 ± 0.003	2	0.034 ± 0.007
K-500	Aged	0.021 ± 0.003	2	0.042 ± 0.007

Figure 1. Dependence of flux on overpotential for Marinel and aged alloy K-500.
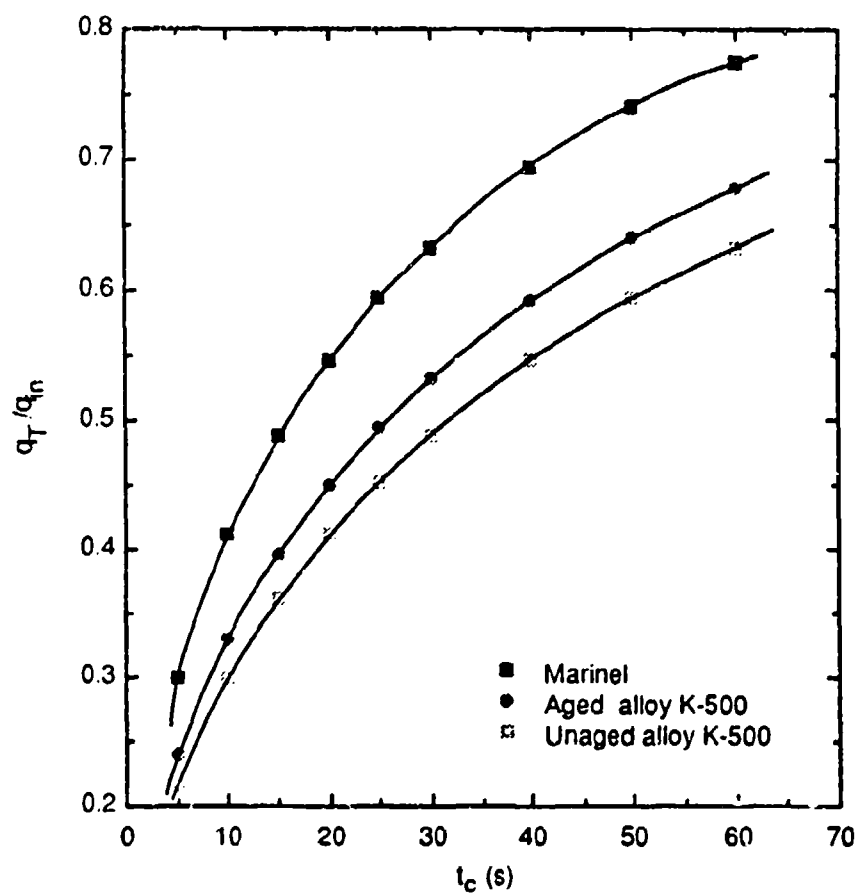
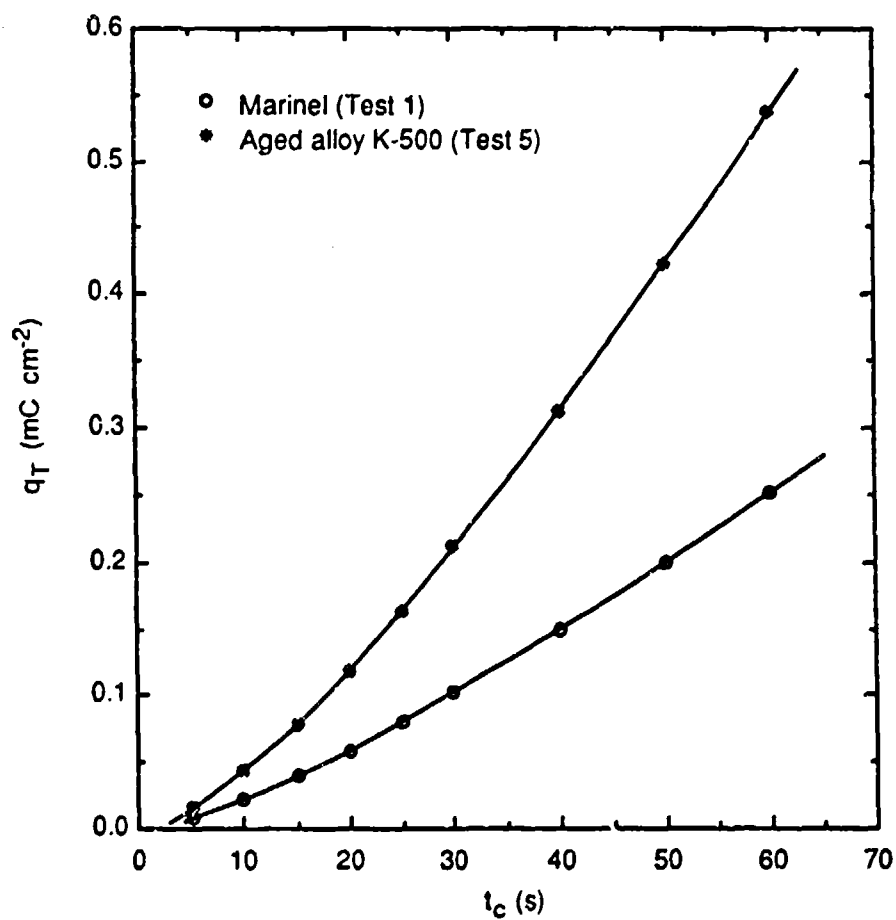Figure 2. Dependence of q_T/q_{in} on charging time for Marinel and aged alloy K-500.

Figure 3. Dependence of q_T on charging time for Marinel and aged alloy K-500.

$\eta = -0.4$ V.

A COMPARISON OF HYDROGEN INGRESS BEHAVIOR
IN ALLOYS 625 AND 716

ABSTRACT

The ingress of hydrogen in a high-strength nickel-base alloy (UNS N07716) exposed to an acetate electrolyte (1 mol L⁻¹ HAc/1 mol L⁻¹ NaAc where Ac = acetate) was studied using a technique referred to as hydrogen ingress analysis by potentiostatic pulsing (HIAPP). Values of the irreversible trapping constant (k) and the hydrogen entry flux were determined for various charging potentials. The density of irreversible trap particles/defects was calculated from k and found to be in agreement with the concentration of Ti-rich carbide particles. Alloy 716 has the highest value of k among a range of nickel-base alloys, indicating that it should be the most susceptible to hydrogen embrittlement. However, the hydrogen entry flux is apparently low enough that the alloy generally does not undergo cracking during exposure in aggressive environments for periods up to 1000 h, despite the high susceptibility imparted by the type of traps present.

INTRODUCTION

Microstructural heterogeneities in alloys provide trapping sites for diffusing hydrogen and so strongly affect the susceptibility of the alloys to hydrogen embrittlement (HE). These traps can be classified as reve .ible or irreversible, according to their energy for trapping hydrogen.[1,2] Irreversible traps are often highly detrimental to the performance of an alloy in a hydrogen environment,[3] so identification of the dominant types of irreversible traps is crucial to characterizing the susceptibility to HE.

Hydrogen trapping has been studied previously for a wide range of alloys by using a technique referred to as hydrogen ingress analysis by potentiostatic pulsing (HIAPP).[4-7] The alloy is charged with hydrogen at a constant potential (E_c) for a time (t_c), after which the potential is stepped anodically, resulting in a current transient with a charge q_a. For all the alloys studied to date, the transients could be analyzed in terms of a diffusion/trapping model involving a constant entry flux; that is, the rate of ingress was found to be controlled by diffusion under the influence of kinetically limited entry. The anodic charge (in C cm⁻²) passed out in this situation is given by[8]

$$q'(\infty) = F J t_c \{1 - e^{-R}/(\pi R)^{1/2} - [1 - 1/(2R)] \mathrm{erf}(R^{1/2})\} \qquad (1)$$

where $R = k_a t_c$, F is the Faraday constant, J is the ingress flux in mol cm^{-2} s^{-1}, and $q'(\infty)$ is equated to q_a. k_a is an apparent trapping constant and is related to the irreversible trapping constant (k) by $k(D_a/D_L)$ where D_a is the apparent diffusivity and D_L is the lattice diffusivity of hydrogen in the metal.

HIAPP has previously been applied to nickel-base alloys of age-hardened types (718 and 925)[5] and work-hardened types (625 and C-276).[6] In the present study, HIAPP was used to investigate hydrogen ingress in Custom Age 625 PLUS† (UNS N07716), which was developed as an age-hardenable alternative to alloy 625.[9] The hydrogen entry and trapping characteristics were obtained for alloy 716 and compared with those for alloy 625, with the objective of relating these characteristics to their HE susceptibilities.

EXPERIMENTAL PROCEDURE

The specimens of alloys 625 and 716 were supplied in the form of rod with diameters of 1.27 cm and 2.54 cm, respectively. The alloy 625 used in the study of work-hardened alloys[6] was received in a hot-finished and annealed condition with a yield strength of 528 MPa, whereas alloy 716 had been age-hardened to a yield strength of 951 MPa. High strength was a required property in this work, so the 716 and 625 specimens were cold-worked 4% and 17%, respectively, to obtain their final yield strengths of 1186 and 1195 MPa. The composition of each alloy is given in Table 1.

The presence of particles in the alloys was investigated using scanning electron microscopy. Alloy 625 is known to form MC-type carbides that are rich in Nb,[10] and the specimen used in the tests on work-hardened alloys was found to have particles containing Ti and Nb. Alloy 716 exhibited Ti-rich carbides. The characteristic dimension of the particles was determined to be 1.2 μm and 2.4 μm for the 716 and 625 specimens, respectively, by taking the mean of the linear dimensions in the exposed plane. The respective particle concentrations were found to be 1.6×10^{15} m^{-3} and 7.4×10^{13} m^{-3}.

Details of the electrochemical cell and instrumentation have been given previously.[4] The test electrodes of each alloy consisted of a 5-cm length of rod press-fitted into a Teflon sheath so that only the planar end surface was exposed to the electrolyte. The surface was polished with SiC paper followed by 0.05-μm alumina powder. The electrolyte was an acetate buffer (1 mol L^{-1} acetic acid/1 mol L^{-1} sodium acetate) containing 15 ppm As_2O_3 as a hydrogen entry promoter. The electrolyte was deaerated with argon for 1 hour before measurements began and throughout data

---

† Trademark of Carpenter Technology Corp., Reading, PA.

acquisition. The potentials were measured with respect to a saturated calomel electrode (SCE). All tests were performed at $22 \pm 1^\circ C$.

The test electrode was charged with hydrogen for times from 5 s to 60 s at a given overpotential ($\eta = E_c - E_{oc}$) and then discharged at a potential 10 mV negative of the open-circuit potential (E_{oc}). Anodic current transients were obtained for each charging time over a range of overpotentials. The open-circuit potential of the test electrode was sampled immediately before each charging time, so that E_c could be established. Sampling E_{oc} also allowed the stability of the surface film to be monitored.

RESULTS

A typical current transient for alloy 716 is shown in Fig. 1. Data for q_a were analyzed using Eq. (1) to determine k_a corresponding to values of J that were independent of charging time. Values of k_a and J for alloys 625 and 716 are given in Table 2. The data shown for alloy 625 were obtained in the study of work-hardened alloys[6] and are presented here for comparison.

The entry flux for alloy 716, like that for alloy 625, increased with potential but was still low when film reduction occurred at sufficiently negative charging potentials. Owing to the low flux, the increase in q_a with charging time was adequately defined only over a relatively narrow potential range. Accordingly, a number of tests were performed to ensure that a reliable value of k_a was obtained. The mean value of k_a was 0.054 s^{-1} with a mean deviation of ± 0.004 s^{-1}. In the case of alloy 625, k_a had a mean value of 0.004 ± 0.002 s^{-1}.

DISCUSSION

Irreversible Trapping Constants

Values of D_L and D_a, corresponding to the diffusivity for the pure Ni-Cr-Mo alloy and for alloy 716 respectively, are required for k to be evaluated. Reversible trapping in alloy 716, as in other fcc alloys,[5,6] is assumed to be associated principally with the minor alloying elements. The most appropriate value of D_L is $(7.9 \pm 1) \times 10^{-15}$ m^2 s^{-1}, which was obtained for 76Ni-16Cr-8Fe.[11] While the compositions of the pure alloy and alloy 716 differ to some degree in the content of their main alloying elements, especially Mo, the error in using the diffusivity of the Ni-Cr-Fe alloy for D_L is assumed to be small.

As with alloy 625, the diffusivity does not appear to be available for alloy 716, so D_a must be estimated from data for similar alloys. The diffusivity of hydrogen at 25°C was estimated to be $(2.1 \pm 0.2) \times 10^{-15}$ m^2 s^{-1} for 5% cold-worked Hastelloy C-276[12] and 2.0×10^{-15} m^2 s^{-1} for Inconel 718 (unaged and aged).[13] Accordingly, a value of $(2.1 \pm 0.2) \times 10^{-15}$ m^2 s^{-1} seems to be

reasonable for alloy 716 in the aged and slightly cold-worked condition. With these values for D_L and D_a, k for alloy 716 is found to be 0.20 ± 0.06. In contrast, the corresponding value for alloy 625 is 0.014 ± 0.010 s^{-1}.

Identification of Traps

The density of particles or defects (N_i) providing irreversible traps can be obtained from k_a by using a model[5,14] based on spherical traps of radius d:

$$N_i = k_a a/(4\pi d^2 D_a) \tag{2}$$

where a is the diameter of the metal atom. The value of d is estimated from the characteristic dimension of particles or defects that are potential irreversible traps. The dominant irreversible trap can then be identified by comparing the trap density with the concentrations of potential traps in the alloy.

The Ti-rich carbide particles were assumed to act as the principal irreversible traps in alloy 716. On the basis of this assumption, the density of irreversible trap particles was calculated by treating the carbide particles as spherical with a mean radius of 0.6 μm. The value of a for alloy 716 was taken as the weighted mean of the atomic diameters of the appropriate alloying elements. By using $D_a = 2.1 \times 10^{-15}$ m^2 s^{-1} and $a = 253 \times 10^{-12}$ m, the density of trap particles was calculated to be 1.4×10^{15} m^{-3}. Despite the uncertainty in D_a for alloy 716 and the assumption that the traps and carbides are spherical, the trap density is in exact agreement with the actual concentration of carbide particles (1.4×10^{15} m^{-3}), corroborating their role as the principal irreversible traps.

Comparison of Trapping Parameters

The irreversible trapping constants for alloy 716 and other hardened nickel-base alloys are summarized in Table 3. The trapping capability, as represented by k, for a wide range of alloys has been shown to parallel their relative susceptibilities to HE.[5-7] On the basis of this correlation, alloy 625 is predicted to be the least susceptible of the four nickel-base alloys, which is consistent with test results that show it to be more resistant to cracking than alloy 718[9] and, as discussed previously,[6] alloy C-276.

In contrast, alloy 716 should be the most susceptible, but cracking tests have indicated that it is comparable to alloy 625 of similar yield strength in being able to withstand exposure in aggressive environments.[9] Although alloy 716 has a high susceptibility in terms of trapping characteristics, the hydrogen concentration at the dominant traps evidently remains below the

4-4

critical level required to initiate cracking. The implication, therefore, is that the apparent resistance of alloy 716 to cracking is associated with the entry flux, which was low in the acetate buffer and was apparently low enough in the cracking test environments to delay failure in most cases (up to 1000 h).

Another factor to be considered is the size of the irreversible trap particles, since a transition in HE susceptibility can occur as a result of a large change in particle size. Bernstein and Pressouyre[3] have argued that a high density of well-dispersed, small («1 μm) particles should improve the resistance to hydrogen-induced cracking, whereas large (>1 μm) particles should be detrimental. The particles in alloy 716 as well as in alloys 718 and 625 all exceeded 1 μm in size, so the cracking resistance of alloy 716 should not result from a dramatic effect of particle size. Accordingly, the primary reason for the ability of alloy 716 to withstand exposure appears to be a low entry flux rather than small particle size.

The magnitude of k, as indicated above, represents the irreversible trapping capability of the principal trap particles or defects in an alloy. For alloys with a similar hydrogen diffusivity (D_a) and atomic size (a), k is predicted on the basis of Eq. (2) to increase linearly with $N_i d^2$. Hence, in the case of the three alloys (625, 716, and 718) containing carbide or carbonitride particles, k should reflect the total surface area of the particles, since they provide the principal irreversible traps. Fig. 2 shows the dependence of k on $C_p(d_c/2)^2$, where C_p is the concentration of particles and d_c is their characteristic dimension. Although the amount of data is limited, it is apparent that a linear relationship exists, which underscores the fact that the carbides/carbonitrides are primarily responsible for irreversible trapping in these alloys.

SUMMARY

Alloy 716, like alloy 625, is characterized by a single type of irreversible trap. The calculated trap density indicated that the principal irreversible traps are Ti-rich carbide particles. Alloy 716 has the highest irreversible trapping constant among a range of nickel-base alloys, which indicates that it should be the most susceptible to HE. However, the entry flux for alloy 716, as with alloy 625, is apparently low enough that the alloy generally does not undergo cracking during exposure in aggressive environments for periods up to 1000 h, despite the high susceptibility imparted by the type of traps present.

ACKNOWLEDGMENTS

REFERENCES

1. I. M. Bernstein and G. M. Pressouyre, in *Hydrogen Degradation of Ferrous Alloys*, R. A. Oriani, J. P. Hirth, and M. Smialowski, Eds. (Noyes Publications, 1985), p. 641.

2. M. Pressouyre, *Metall. Trans.* **10A**, 1571 (1979).

3. G. M. Pressouyre and I. M. Bernstein, *Acta Metall.* **27**, 89 (1979).

4 B. G. Pound, *Corrosion* **45**, 18 (1989).

5. B. G. Pound, *Acta Metall.* **38**, 2373 (1990).

6. B. G. Pound, *Acta Metall.* **39**, 2099 (1991).

7. B. G. Pound, *Corrosion* **47**, 99 (1991).

8. R. McKibbin, D. A. Harrington, B. G. Pound, R. M. Sharp, and G. A. Wright, *Acta Metall.* **35**, 253 (1987).

9. R. B. Frank and T. A. DeBold, "Properties of an Age-Hardenable, Corrosion-Resistant Nickel-Base Alloy," Corrosion 88, Paper No. 75, (National Association of Corrosion Engineers, Houston, Texas, 1988).

10. *Inconel alloy 625*, Inco Alloys International (Huntington, West Virginia, 1985).

11. M. Cornet, C. Bertrand, and M. Da Cunha Belo, *Metall. Trans.* **13A**, 141 (1982).

12. D. A. Mezzanotte, J. A. Kargol, and N. F. Fiore, *Metall. Trans.* **13A**, 1181 (1982).

13. W. M. Robertson, *Metall. Trans.* **8A**, 1709 (1977).

14. B. G. Pound, R. M. Sharp, and G. A. Wright, *Acta Metall.* **35**, 263 (1987).

Table 1
ALLOY COMPOSITION (wt%)

Element	Alloy 625	Alloy 716
Al	0.18	0.22
C	0.03	0.011
Co		<0.01
Cr	22.06	20.99
Fe	4.37	5.32
Mn	0.17	0.01
Mo	8.70	8.10
Nb+Ta	3.50	3.47
Ni	60.33	60.50
P	0.012	0.004
S	0.001	0.001
Si	0.38	0.02
Ti	0.27	1.35

Table 2
VALUES OF k_a AND J FOR ALLOYS 625 AND 716

Alloy	Test	η (V)	E_c (V/SCE)	k_a (s^{-1})	J (nmol cm^{-2} s^{-1})
625	1	-0.200	-0.355	0.006	0.01
	2	-0.100	-0.391	0.001	0.01
	3	-0.100	-0.378	0.004	0.01
		-0.150	-0.433	0.002	0.02
	4	-0.050	-0.427	0.008	0.03
716	1	-0.150	-0.421	0.056	0.046
	2	-0.100	-0.380	0.054	0.026
	3	-0.150	-0.357	0.043	0.020
		-0.175	-0.387	0.050	0.032
	4	-0.100	-0.377	0.050	0.021
	5	-0.150	-0.348	0.055	0.022
	6	-0.075	-0.340	0.059	0.014
		-0.150	-0.398	0.055	0.035
	7	-0.100	-0.351	0.058	0.017
		-0.150	-0.386	0.058	0.029

Table 3
TRAPPING PARAMETERS

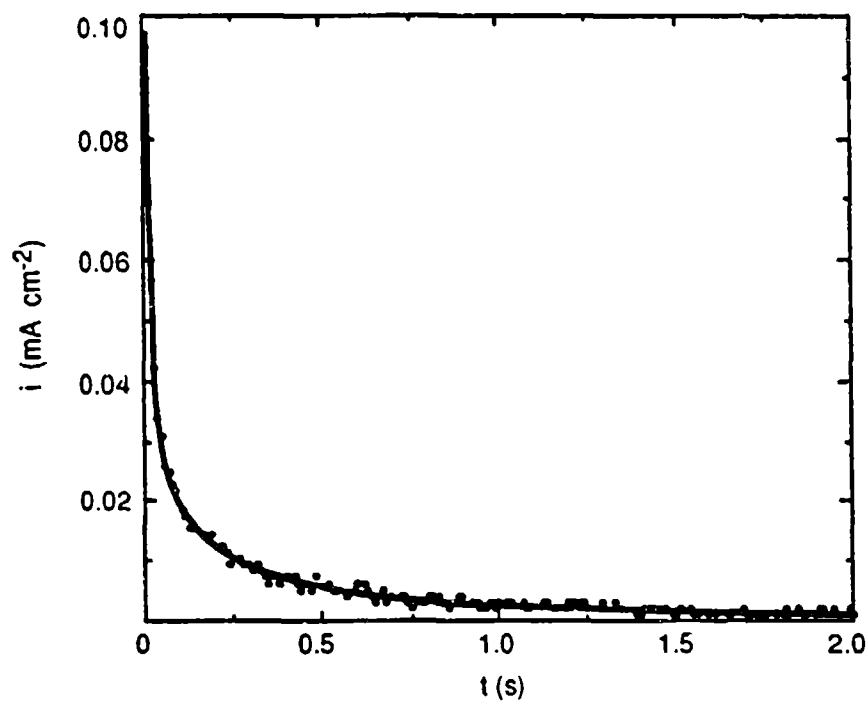| Alloy	Yield Strength (MPa)	k_a (s^{-1})	D_L/D_a	k (s^{-1})
716 (4% cw)[a]	1186	0.054 ± 0.004	3.8 ± 0.8	0.20 ± 0.06
718	1238	0.031 ± 0.002	4.0 ± 0.5	0.128 ± 0.024
C-276 (27% cw)	1237	0.025 ± 0.003	3.6 ± 0.8	0.090 ± 0.030
		0.019 ± 0.010[b]	3.6 ± 0.8	0.068 ± 0.051[b]
625 (17% cw)	1195	0.004 ± 0.002	3.6 ± 0.8	0.014 ± 0.010

[a] cw = Cold-work
[b] Quasi-irreversible trapping

Figure 1. Anodic current transient for alloy 716 in an acetate buffer.
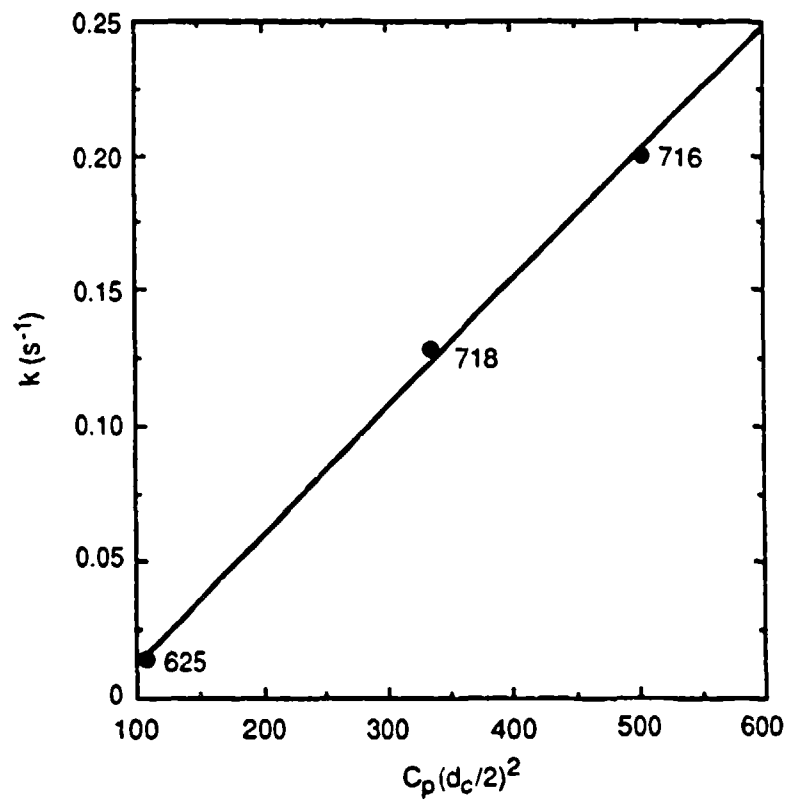t_c = 15 s; E_c = -0.386 V (SCE).

The full transient is not shown.

Figure 2. Dependence of k on $C_p(d_c/2)^2$ for high-strength nickel-base alloys 625, 716, and 718.

PREDICTING THE SUSCEPTIBILITY TO HYDROGEN EMBRITTLEMENT

ABSTRACT

The susceptibility of an alloy to hydrogen embrittlement (HE) is critically affected by the trapping of hydrogen at microstructural defects, so a knowledge of the trapping characteristics is crucial in predicting the susceptibility to HE. Hydrogen trapping in various high-strength steels, precipitation-hardened and work-hardened nickel-base alloys, and titanium has been investigated using a technique referred to as hydrogen ingress analysis by potentiostatic pulsing (HIAPP). HIAPP was found to be effective in evaluating the irreversible trapping characteristics of alloys containing both single and multiple principal traps. The results showed that a range of microstructural features can be identified as the principal irreversible traps and so demonstrated the ability of HIAPP to provide a basis for explaining differences in the resistance of alloys to HE. Furthermore, it was established that the irreversible trapping capability of the alloys can be correlated with the susceptibility to embrittlement. Hence, HIAPP appears to provide a convenient means of quantitatively characterizing the propensity of an alloy to undergo HE.

INTRODUCTION

The susceptibility of an alloy to hydrogen embrittlement (HE) is highly dependent on the interaction of hydrogen with microstructural defects such as precipitates, grain boundaries, and dislocations. These defects provide potential trapping sites for hydrogen and so critically influence the series of events leading to failure. The accumulation of hydrogen at second-phase particles and precipitates, for example, is generally considered to promote microvoid initiation via the fracture of particles or the weakening of particle-matrix interfaces. Traps with a large saturability and a high binding energy for hydrogen are highly conducive to HE,[1,2] whereas metals containing a high density of well-distributed strong traps (high binding energy) that have a low specific saturability should be more resistant. Accordingly, a knowledge of the trapping characteristics is crucial in predicting the susceptibility to embrittlement.

The approach currently used to assess HE susceptibility is based on time-to-failure results from mechanical cracking tests. The disadvantage of these tests is that they require exposure times typically of days or longer and are often laborious. Furthermore, the results are at best only

semiquantitative, and it is frequently difficult, if not impossible, to discriminate between more resistant alloys that do not fail within the given test period.

Over the last few years, hydrogen trapping in various high-strength alloys has been investigated in our laboratory by using an electrochemical technique referred to as hydrogen ingress analysis by potentiostatic pulsing (HIAPP).[3-6] As the name indicates, the alloy of interest is subjected to a potentiostatic pulse and the resulting current transients are analyzed by using a model for hydrogen diffusion and trapping.[7,8] Test data can be acquired rapidly (typically within a few hours) for a range of charging potentials by using only small bulk samples of an alloy. In addition, the data yield both the hydrogen trapping constants and the rates of hydrogen entry into the alloy. A crucial finding was that the hydrogen trapping constants represent an index of HE susceptibility, and so it was shown that HIAPP can provide two key parameters required to characterize the performance of an alloy in an environment conducive to HE.

HIAPP has been applied to high-strength steels,[3,4] precipitation-hardened and work-hardened nickel-base alloys,[4,5] and titanium[6] and was found to be effective in evaluating the trapping characteristics of alloys containing both single and multiple principal traps. This paper reviews the use of HIAPP as a technique for examining hydrogen ingress, particularly in terms of irreversible trapping. The research was aimed at not only characterizing the susceptibility to HE but also, wherever possible, identifying the dominant type of irreversible trap in different alloys. In essence, the goal was to use the data provided by HIAPP as a basis for explaining differences in the resistance of these alloys to HE.

ROLE OF HIAPP

Techniques

Membrane permeation methods have been used extensively to determine diffusion and trapping characteristics, but they suffer from several disadvantages, as discussed elsewhere.[9] Long charging times (on the order of days) may be required for hydrogen to diffuse through many metals, especially those with a fcc lattice, and the likelihood of changes in the surface condition is thereby increased. If a surface film is present, progressive thinning of the film may result from reduction, and the bare metal may eventually be exposed. Prolonged charging times may also result in deposition of significant amounts of impurities on the cathode surface.

A further disadvantage is that most, if not all, diffusion/trapping models for permeation techniques are based on an input boundary condition of constant concentration, which implies that they are strictly applicable only for charging conditions without any entry limitation. Hence, existing permeation models may well yield incorrect values of diffusivity and trapping parameters

if the prevailing boundary condition involves a constant or time-dependent flux. Unfortunately, the limitations of the constant concentration condition are not always recognized, even though it underlies virtually all permeation analyses involving trapping.

In the potentiostatic pulse technique, the metal is cathodically charged with hydrogen for a certain time, t_c, and the potential is then stepped to a more positive value, resulting in an anodic current transient associated with the reoxidation of H atoms as they diffuse back to the same surface. Pulse methods are suitable for bulk specimens, since only a single surface need be exposed to the electrolyte. Hence, they offer practical advantages over permeation methods in terms of specimen shape and charging times. Also, diffusion in bulk specimens can be treated in terms of a semi-infinite boundary condition, which is mathematically appealing.

Diffusion/Trapping Model For Pulse Technique

A model has been developed to allow for the effect of trapping on diffusion without *or* with surface constraints; that is, for cases involving either constant concentration or constant flux at the input surface. These two cases are characterized by the kinetics of hydrogen entry into the metal: (1) pure diffusion control, in which hydrogen entry is assumed to be fast enough that equilibrium is rapidly achieved between adsorbed and subsurface hydrogen; and (2) interface-limited diffusion control (referred to simply as interface control), in which the rate of hydrogen ingress is controlled by diffusion but the entry flux of hydrogen across the interface is restricted.

The interface control model was found to be applicable for all alloys studied to date. According to this model, the total charge passed out is given in nondimensional form by[7]

$$Q'(\infty) = \sqrt{R}\{1 - e^{-R}/\sqrt{(\pi R)} - [1 - 1/(2R)]\mathrm{erf}\sqrt{R}\} \tag{1}$$

The nondimensional terms are defined by $Q = q/[F J\sqrt{(t_c/k_a)}]$ and $R = k_a t_c$, where q is the dimensionalized charge in C cm^{-2}, F is the Faraday constant, and J is the ingress flux in mol cm^{-2} s^{-1}. The charge $q'(\infty)$ corresponding to $Q'(\infty)$ is equated to the charge (q_a) associated with the experimental anodic transients; the adsorbed charge is almost invariably found to be negligible, so q_a can be associated entirely with absorbed hydrogen. k_a is an apparent trapping constant measured for irreversible traps in the presence of reversible traps and can be expressed by $k(D_a/D_L)$ where k is the irreversible trapping constant, D_a is the apparent diffusivity, and D_L is the lattice diffusivity of hydrogen in the metal.

Eq. (1) was fitted to data for q_a as a function of t_c to obtain values of k_a and J such that J was constant over the range of charging times and k_a was independent of charging potential, as is

required for the diffusion/trapping model to be valid, since the traps are assumed to be unperturbed by electrochemical variables and remain unsaturated. The values of k_a and J can be used to calculate the irreversibly trapped charge (q_T) given nondimensionally by

$$Q_T = [R^{1/2} - 1/(2R^{1/2})]erf(R^{1/2}) + e^{-R}/\pi^{1/2} \qquad (2)$$

The charge associated with the entry of hydrogen into the metal (q_{in}) can be determined from its nondimensional form of $Q_{in} = \sqrt{R}$ by using the value of k_a. The data for q_{in}, q_T, and the cathodic charge (q_c) can then be used to obtain two ratios: (1) the trapping efficiency (q_T/q_{in}), corresponding to the fraction of hydrogen trapped in the metal; and (2) the entry efficiency (q_{in}/q_c), representing the fraction of hydrogen entering the metal during charging.

Trap Density

The density of particles or defects (N_i) providing irreversible traps can be obtained from the apparent trapping constant by using a model[4,8] based on spherical traps:

$$N_i = k_a a/(4\pi d^2 D_a) \qquad (3)$$

where a is the diameter of the metal atom and d is the trap radius, which is estimated from the dimensions of heterogeneities that are potential irreversible traps. The value of a for an alloy is taken as the mean of the atomic diameters weighted in accordance with the atomic fraction of each element. The predominant irreversible trap can be identified by comparing the calculated trap density with the actual concentrations of specific heterogeneities in the alloy.

The assumption of spherical traps is an approximation in most cases. However, for various alloys studied to date, the calculated trap densities have shown close agreement with the concentrations of potential trap particles that are clearly not spherical, which suggests that use of a more applicable trap geometry would make little difference in identifying the principal traps.

EXPERIMENTAL

The composition and yield strength of each alloy are given in Tables 1 and 2, respectively. Table 2 also shows the thermomechanical treatment used for each alloy. A number of the alloys contained micrometer-sized particles such as carbides or, in the case of 4340 steel, sulfide inclusions. The characteristic dimension of these particles was determined as the mean of the linear dimensions in the exposed plane.

The test electrodes of each alloy consisted of a length (1.3-3.8 cm) of rod press-fitted into a Teflon sheath so that only the planar end surface was exposed to the electrolyte. The surface was polished before each experiment with SiC paper followed by 0.05-μm alumina powder. The electrolyte was an acetate buffer (1 mol L^{-1} acetic acid/1 mol L^{-1} sodium acetate) containing 15 ppm As_2O_3 as a hydrogen entry promoter. The electrolyte was deaerated with argon for 1 h before measurements began and throughout data acquisition. The potentials were measured with respect to a saturated calomel electrode (SCE). All tests were performed at 22 $\pm$ 2°C. Details of the electrochemical cell and instrumentation have been given elsewhere.[3]

The test electrode was charged with hydrogen at a constant potential E_c for a time t_c, after which the potential was stepped in the positive direction to a value 10 mV negative of the open-circuit potential E_{oc}.[3,7,8] Anodic current transients with a charge q_a were obtained over a range of charging times (0.5-60 s) at different overpotentials ($\eta = E_c - E_{oc}$). The open-circuit potential of the test electrode was sampled immediately before each charging time and was also used to monitor the stability of the surface oxide; reduction of the film was evident from a progressive shift of E_{oc} to more negative values with each t_c at a sufficiently high charging potential. A typical transient is shown in Figure 1. Experimental and fitted values of q_a for various charging times are compared in Figure 2, which illustrates the level of agreement obtained for the alloys in this work.

INITIAL APPLICATION OF HIAPP

The application of HIAPP to alloys was explored initially with a high-strength steel — AISI 4340 (UNS G43400), and two nickel-containing alloys — Monel K-500 (UNS N05500) and MP35N (UNS R30035).[3] The aim was to determine their hydrogen ingress characteristics and compare them in relation to differences in their HE susceptibility.

Hydrogen Ingress Characteristics

The values of k_a and k are shown in Table 3. k_a was found to be independent of heat treatment in the case of 4340 steel. Initial results[3] for alloy K-500 indicated that there was no apparent difference in trapping behavior between the unaged and aged alloy, but improvements in data aquisition have since revealed that the trapping constant of the aged alloy is a little higher than that of the unaged alloy.[10]

The values of both k and J are higher for 4340 steel than those for alloys K-500 and 35N. Hence, both of these parameters are consistent with the steel being more susceptible to HE than the two nickel-containing alloys. The reduction of H^+ and subsequent entry of H atoms into alloys K-500 and 35N occurred on an oxide-covered surface, which undoubtedly explains the lower

hydrogen flux for these alloys. Perhaps of more significance in terms of susceptibility is the nature of the irreversible traps reflected by the values of k. This issue was explored further by calculating the density of irreversible trap defects (commonly second-phase particles and precipitates) from k_a [Eq. (3)] and comparing it with the actual defect concentration in the alloy.

Identification of Traps

4340 Steel. The trap density was calculated in terms of MnS inclusions and was found to be in reasonable agreement with the actual concentration of these inclusions, which indicates that they did indeed provide the primary irreversible traps in this alloy. The lack of change in k_a — and therefore N_i — with heat treatment was further evidence that the irreversible traps were associated with some stable species such as MnS inclusions.

Alloys K-500 and 35N. HE in Ni-Cu base alloys and alloy 35N is known to be assisted by sulfur and phosphorus segregated at grain boundaries.[11,12] Since hydrogen also probably segregates to the grain boundaries as in Ni,[13] grain boundary S and P were assumed to provide the irreversible traps predominantly encountered by hydrogen in alloys K-500 and 35N. However, a lack of data for S and P segregation in these alloys makes it difficult to verify the nature of the traps by the approach used here.

The density of irreversible traps provided by atomic S and P is 3 orders of magnitude less than the overall S and P content determined from the alloy composition (Table 1). Hence, it is clear that, provided that S and P are the principal irreversible traps, any useful comparison of N_i must be made with respect to grain boundary concentrations. Subsequent work[5] on Hastelloy C-276 (UNS N10276) has shown that it is possible for the trap density to agree closely with the amount of grain boundary P distributed per unit volume of the alloy. Hence, it does seem reasonable in the case of alloys K-500 and 35N to consider S and P at grain boundaries, rather than in the bulk alloy, to be the primary irreversible traps.

Rationale for HE Susceptibility

Two significant findings emerged from this work in terms of rationalizing differences in the HE susceptibility of the three alloys. First, values of k and J for 4340 steel were higher than those for alloys K-500 and 35N. Second, the irreversible traps in the steel appeared to be associated with inclusions, whereas those in alloys K-500 and 35N were considered to be elements segregated at grain boundaries. The difference in both the nature of the irreversible traps and the interfacial flux must play a major role in the different susceptibilities of the steel and the two Ni-containing alloys. The sulfide inclusions, in particular, can be linked to the susceptibility of 4340

steel, since they are strong traps with a large hydrogen capacity; in other words, these inclusions possess the two characteristics that are most detrimental.

FURTHER APPLICATION OF HIAPP

The application of HIAPP was extended to alloys of various groups: Precipitation-hardened alloys — Inconel 718 (UNS N07718), Incoloy 925 (UNS N09925), and 18Ni maraging steel;[4] work-hardened alloys — Inconel 625 (UNS N06625) and Hastelloy C-276;[5] and pure (99.99%) and grade 2 (UNS R50400) titanium.[6] In the case of pure Ti, the anodic charge was invariant with t_c, indicating that negligible hydrogen enters the metal. The resistance of pure Ti to hydrogen entry was attributed to the surface film, which is known to be a highly effective barrier.

Hydrogen Ingress Characteristics

The mean values of k_a and k are summarized in Table 3. The maraging steel has the highest value of k, followed by alloys 718, C-276, and 925, Ti grade 2, and alloy 625. Stress-rupture tests during electrolytic charging have shown that 18Ni (1723 MPa) maraging steel undergoes severe embrittlement, whereas alloy 718 exhibits negligible susceptibility.[14] In addition, test results suggest that Incoloy 903 (UNS N09903)[15] and, by implication, alloy 925 are less sensitive than alloy 718[14] to HE. Hence, the irreversible trapping constants for the precipitation-hardened alloys are consistent with their relative susceptibilities to HE.

A similar comparison of the susceptibilities of alloys C-276 and 625 is complicated by their sensitivity to the amount of cold work performed in each case. However, the ranking of these alloys can be determined indirectly from previous studies of alloys C-276 and G (UNS N06007).[16] The comp sition of alloy G is comparable to that of alloy 625, and it can be reasoned[5] that, for the degree of cold work involved, alloy C-276 should be more susceptible to embrittlement, as indeed is indicated by the trapping constants. The susceptibility of alloy C-276 relative to the other alloys, as reflected by its trapping constant, is subject to some question because of the uncertainty in k.

Titanium grade 2 exhibited two values of k, depending on the level of hydrogen present in the metal. The similarity in trapping constants for Ti grade 2 and alloy 925 fits their relative resistance to HE in that long exposure times are required for the concentration of hydrogen to exceed the level necessary to result in a loss of mechanical properties.[15,17] Furthermore, the higher trapping constant coincides with the increasing susceptibility to embrittlement with hydrogen concentration as a result of hydride precipitation.

Identification of Traps

Alloy 718. The irreversible traps were assumed to be niobium carbide particles, and the density of trap particles was calculated to be 2.0×10^{13} m^{-3}, as compared with 2.2×10^{13} m^{-3} for the actual concentration of carbide particles. This close agreement was remarkable in view of the spherical shape assumed for the traps and carbides, but it indicates clearly that large traps with both a high surface area and a high trapping energy can overwhelmingly dominate the irreversible trapping behavior of an alloy.

Alloy 925. TiC particles were assumed to provide the irreversible traps in Incoloy 925, and the density of trap particles was calculated to be 4.1×10^{13} m^{-3}. The actual concentration of carbide particles (4.6×10^{13} m^{-3}) and the trap density were again found to be in close agreement, despite both the traps and carbides being treated as spherical.

18Ni Maraging Steel. A combination of irreversible traps and quasi-irreversible traps appeared to be present in this alloy. The quasi-irreversible traps were difficult to identify, although autoradiography studies have shown that trapping occurs at grain boundaries and martensite boundaries in maraging steel.[18] Both sites appear to be moderately strong traps. However, grain boundaries are generally considered to be reversible traps in ferritic steels, and so the martensite boundaries may well be stronger traps. The martensite boundaries, like grain boundaries,[19] were assumed to have an influence diameter of 3 nm, which gave a trap density of 9×10^{17} m^{-3}.

The irreversible traps were able to be identified more closely, with qualified support coming from the comparison of N_i with particle concentration. Trapping has been observed at carbo-nitride interfaces in maraging steels,[18] and so the density of irreversible traps was calculated on the basis of TiC/Ti(CN) particles. N_i was calculated to be 3.4×10^{11} m^{-3}, as compared with $(1.1 \pm 0.6) \times 10^{13}$ m^{-3} for the actual concentration of particles. The two values differ by a factor of ~30, which can largely be accounted for by uncertainties in both the concentration of particles and the value of D_a assumed for the maraging steel. In view of these uncertainties, the calculated trap density and carbide/nitride concentration were considered to correlate moderately well.

Alloy 625. In this alloy, NbTi carbide particles were assumed to act as the principal irreversible traps, and the density of trap particles was calculated to be 2.5×10^{13} m^{-3}. Since there was some uncertainty in D_a for this alloy, the trap density was regarded as being in good agreement with the actual concentration of particles (7.4×10^{13} m^{-3}).

Alloy C-276. The trapping behavior can be interpreted on a basis similar to that for 18Ni maraging steel, in which both irreversible and quasi-irreversible traps exist. The quasi-irreversible trapping was consistent with the formation of an unstable hydride during charging. In the

irreversible case, the traps were clearly different from those in the other cold-worked alloy (625), since carbide particles appeared to be absent in alloy C-276. The HE susceptibility of this alloy, like that of alloy 35N, has been correlated with the concentration of phosphorus segregated at grain boundaries.[20] Hydrogen probably segregates to the grain boundaries also in this case, so grain boundary P was again assumed to provide the irreversible traps. It should be noted that, although P may play a role in alloy 625, the carbide particles appear to dominate the irreversible trapping.

The concentration of grain boundary P was estimated on the basis of a simple microstructural model involving cubic grains of length b (in m).[5] By using data for P enrichment at grain boundaries in alloy C-276,[20] it was shown that the amount of grain boundary P per unit volume (C_b) is given by $9 \times 10^{16}/b$ atoms m^{-3}. The value of b for the C-276 alloy was estimated to be 10 μm, and therefore, C_b was calculated to be $\sim 9 \times 10^{21}$ P atoms m^{-3}. In contrast, the total P content of the alloy corresponded to 8.6×10^{24} atoms m^{-3}, while the trap density calculated on the basis of atomic P was found to be 1.9×10^{22} m^{-3}. The close agreement between the values of C_b and N_i was somewhat fortuitous but demonstrated that grain boundary P can in fact provide the primary irreversible traps.

Titanium Grade 2. For Ti grade 2, the increase in trapping constant at a high enough overpotential can be ascribed to an additional type of irreversible trap participating concurrently with the irreversible traps detected at low overpotentials. The trap density at low hydrogen levels was calculated in terms of the minor elements (C, N, O, and Fe), and it was found that all of them except nitrogen could be discounted as the principal irreversible trap. Interestingly, among the interstitials, nitrogen is particularly effective in reducing the ductility of titanium,[21] which coincides with its apparent role as the principal trap. Hence, nitrogen may strongly affect the susceptibility of Ti grade 2 to HE through its combined influence on brittleness and hydrogen trapping.

The additional trapping constant obtained at high hydrogen levels [$E_c < -0.93$ V(SCE)] is probably associated with the accelerated formation of hydrides reported[22] to occur at potentials more negative than -1.0 V (SCE). A decrease observed in the hydrogen entry efficiency (Figure 3) in this potential region is consistent with the presence of a partial barrier to hydrogen entry and so provides support for the formation of a thick hydride layer.

Rationale for HE Susceptibility

Two key features marked the work extending the use of HIAPP. First, the trapping capability of the individual alloys was shown to be consistent with their relative susceptibilities to HE. Second, a range of microstructural features were identified as the predominant irreversible traps, present as either a single type or multiple types.

Alloys 625, 718, and 925 were each characterized by a single type of irreversible trap — (NbTi)C, NbTi(CN), and TiC particles, respectively — whereas alloy C-276 and 18Ni maraging steel were characterized by both an unidentified quasi-irreversible trap and an irreversible trap thought to be grain boundary phosphorus in the case of alloy C-276 and TiC/Ti(CN) particles in the case of the steel. Ti grade 2 exhibits two types of irreversible trap — probably involving interstitial nitrogen and hydride formation — depending on the concentration of hydrogen in the metal. The type of trap defect tends to be reflected by its size, so the type, together with the defect concentration (N_i) and the hydrogen diffusivity, determines the magnitude of k.[4] Thus, in view of the diversity of microstructural features that act as the predominant traps, it is not surprising that the HE susceptibility varies considerably between alloys.

RANKING SUSCEPTIBILITY TO HYDROGEN EMBRITTLEMENT

The irreversible trapping constants for all the alloys tested in this work are listed in Table 4 in descending order. Clearly, there is a strong correlation between the HE susceptibility and the trapping capability of the alloy as represented by k. The trapping constants, as might be expected, indicate that the 4340 steel is the most susceptible, followed by the maraging steel, which is predicted to be somewhat less so on the basis of its k. The sequence of k values for the two steels is in agreement with experimental results, which showed that 4340 steel was more susceptible to hydrogen-induced cracking than 18 Ni(250) maraging steel.[23] At the other extreme, the low trapping constant for alloy 35N is consistent with the high resistance to HE found in practice for this alloy.[24]

Because of a lack of relevant results for HE, it is difficult to determine whether the two cold-worked alloys follow the observed pattern for the trapping constants. Moreover, some uncertainty in the values of k for alloys C-276 and 625 compounds the difficulty of evaluating the position of these alloys in Table 3, beyond noting that, as discussed above, the C-276 alloy in this study is somewhat more susceptible to embrittlement than alloy 625. The position of alloy 625 is comparable to that of alloy 35N within the uncertainty of k. Failure tests[24] indicate that alloy 625 with 17% cold work should be at least as resistant to HE as alloy 35N in the condition of interest (40% cold reduced and aged) in our work. In fact, the Inconel may be more resistant than the alloy 35N specimen, as implied by their different values of k. Hence, the trapping constants of alloys 625 and 35N appear to be consistent with the relative HE susceptibilities.

SUMMARY

A correlation was shown to exist between trapping capability and HE susceptibility for a wide range of alloys. In the case of 4340 steel and 18Ni maraging steel, the trapping constants reflect their relatively high susceptibility, whereas the nickel-base alloys display less trapping capability than the two steels and, as expected, are observed to be more resistant to HE. Differences in the resistance of the nickel-b⌐ ╵ alloys are smaller than those for the steels, but they can still be resolved from the trapping constants. In particular, the trapping constants for alloys within groups defined by thermomechanical treatment (precipitation- and work-hardening) are consistent with their relative susceptibilities to embrittlement. Thus, HIAPP appears to provide a convenient means of quantitatively characterizing the susceptibility of an alloy to HE. In addition, a range of microstructural features can be identified as the predominant irreversible traps, either singly or in the presence of multiple principal traps.

ACKNOWLEDGMENT

REFERENCES

1. G. M. Pressouyre and I. M. Bernstein, Metall. Trans., **9A** (1978): p. 1571.

2. G. M. Pressouyre and I. M. Bernstein, Acta Metall., **27** (1979): p. 89.

3 B. G. Pound, Corrosion, **45** (1989): p. 18.

4. B. G. Pound, Acta Metall., **38** (1990): p. 2373.

5. B. G. Pound, Acta Metall., **39** (1991): p. 2099.

6. B. G. Pound, Corrosion, **47** (1991): p. 99.

7. R. McKibbin, D. A. Harrington, B. G. Pound, R. M. Sharp, and G. A. Wright, Acta Metall., **35** (1987): p. 253.

8. B. G. Pound, R. M. Sharp, and G. A. Wright, Acta Metall., **35** (1987): p. 263.

9. B. G. Pound, in *Modern Aspects of Electrochemistry*, J. O'M. Bockris, B. E. Conway, and R. E. White, Eds., No. 25, in press (Plenum Press, New York).

10. B. G. Pound, Corrosion, submitted for publication.

11. J. D. Fransen and H. L. Marcus, in *Effect of Hydrogen on the Behavior of Materials*, I. M. Bernstein and A. W. Thompson, Eds. (Warrendale, PA: The Metallurgical Society of AIME, 1976), p. 233.

12. R. D. Kane and B. J. Berkowitz, Corrosion, **36** (1980): p. 29.

13. D. H. Lassila and H. K. Birnbaum, Acta Metall., **35** (1987): p. 1815.

14. R. J. Walter, R. P. Jewett, and W. T. Chandler, Mater. Sci. Eng., **5** (1969/70): p. 98.

15. C. G. Rhodes and A. W. Thompson, Metall. Trans., **8A** (1977): p. 949.

16. D. A. Mezzanotte, J. A. Kargol, and N. F. Fiore, Metall. Trans., **13A** (1982): p. 1181.

17. R. W. Schutz and D. E. Thomas, in *Metals Handbook*, 9th ed., Vol. 13 (Metals Park, OH: American Society for Metals, 1987), p. 669.

18. M. Aucouturier, G. Lapasset, and T. Asaoka, Metallography, **11** (1978): p. 5.

19. M. Pressouyre, Metall. Trans., **10A** (1979): p. 1571.

20. B. J. Berkowitz and R. D. Kane, Corrosion, **36** (1980): p. 24.

21. A. E. Jenkins and H. W. Worner, J. Inst. Metal., **80** (1951/52): p. 157.

22. H. Sato, T. Fukuzuka, K. Shimogori, and H. Tanabe, in *Proceedings of the Second International Congress on Hydrogen in Metals*, **3** (Paris, 1977).

23. T. P. Groeneveld, E. E. Fletcher, and A. R. Elsea, "A Study of Hydrogen Embrittlement of Various Alloys," Tech. Support Package to Tech. Brief No. 67-10141 (Washington D.C.: NASA, 1967), p. 135.

24. R. D. Kane, M. Watkins, D. F. Jacobs, and G. L. Hancock, Corrosion, **33** (1977): p. 309.

Table 1
ALLOY COMPOSITION (wt%)

Alloy	Al	C	Co	Cr	Cu	Fe	Mn	Mo	Ni	P	S	Si	Ti	Other
4340 steel	0.031	0.42		0.89	0.19	bal	0.46	0.21	1.74	0.009	0.001	0.28		0.005 N, 0.001 O, 0.05 Ca
18Ni steel	0.13	0.009	9.15	0.06	0.11	bal	0.01	4.82	18.42	0.004	0.001	0.04	0.65	0.003 B, 0.01 W, 0.02 Zr
K-500	2.92	0.16			29.99	0.64	0.72		64.96		0.001	0.15	0.46	
35N		0.003	bal	20.19		0.34	<0.01	9.55	35.88	0.003	0.002	0.02	0.85	
7t8	0.60	0.03	0.16	18.97	0.04	16.25	0.10	3.04	54.41	0.009	0.002	0.11	0.98	0.003 B, 5.30 Nb+Ta
925	0.30	0.02		22.20	1.93	28.96	0.62	2.74	40.95		0.001	0.17	2.11	
C-276		0.002	0.83	15.27		5.84	0.48	16.04	57.5	<0.005	<0.002	<0.02		3.90 W
625	0.18	0.03		22.06		4.37	0.17	8.70	60.33	0.012	0.001	0.38	0.27	0.12 V, 3.50 Nb+Ta
Ti grade 2		0.021				0.17							bal	0.007 N, 0.16 O, <0.005 H

Table 2
Thermo-Mechanical Treatment of Alloys

Alloy	Heat Treatment[a]	Test Condition	Yield Strength (MPa)
4340 steel	Annealed	Austenized/tempered to HRC 41 and 53	1206 &1792
18Ni steel	Aged (482°C, 4 h)	As received	1954
K-500	Cold drawn, unaged	As received / Aged (600°C, 8 h)	758 / 1096
35N	Cold drawn and aged	As received	1854
718	Hot finish, solution treated	As received	1238
925	Hot finish, annealed, aged	As received	758
625	Hot finish, annealed	17% cold work	1195
C-276	Hot rolled	27% cold work	1237
Ti Grade 2	Annealed (620°C, 1 h)	As received	380

[a] Provided by producer.

Table 3
Trapping Parameters

Alloy	k_a (s^{-1})	D_L/D_a	k (s^{-1})
4340 steel	0.008 ± 0.001	500	4.0 ± 0.5
K-500 Unaged	0.017 ± 0.003	2.0	0.034 ± 0.006
Aged	0.021 ± 0.003	2.0	0.042 ± 0.006
35N	0.026 ± 0.002	1	0.026 ± 0.002
718	0.031 ± 0.002	4.0 ± 0.5	0.124 ± 0.024
925	0.006 ± 0.003	4.6 ± 0.6	0.034 ± 0.004
18Ni steel	0.005 ± 0.002	300 ± 90	1.50 ± 1.05
	0.010 ± 0.005[a]	300 ± 90	3.00 ± 2.40
625	0.004 ± 0.002	2.6 ± 0.8	0.014 ± 0.010
C-276	0.025 ± 0.003	2.6 ± 0.8	0.090 ± 0.030
	0.019 ± 0.010[a]	2.6 ± 0.8	0.068 ± 0.051
Ti pure	na[b]	1	na
Ti grade 2	0.028 ± 0.002	1	0.028 ± 0.002
	0.012 ± 0.006[c]	1	0.012 ± 0.006

[a] Quasi-irreversible trapping; [b] na = not available; [c] Hydride formation.

Table 4
Irreversible Trapping Constants

Alloy	k (s^{-1})
4340 steel	4.0 ± 0.5
18Ni (300) steel	1.50 ± 1.05
718	0.128 ± 0.024
C-276 (27% cw[a])	0.090 ± 0.030
K-500	0.040 ± 0.010
Ti grade 2 (high H)	0.040 ± 0.008
925	0.034 ± 0.004
Ti grade 2 (low H)	0.028 ± 0.002
35N	0.026 ± 0.002
625 (17% cw)	0.014 ± 0.010

[a]cw = cold work
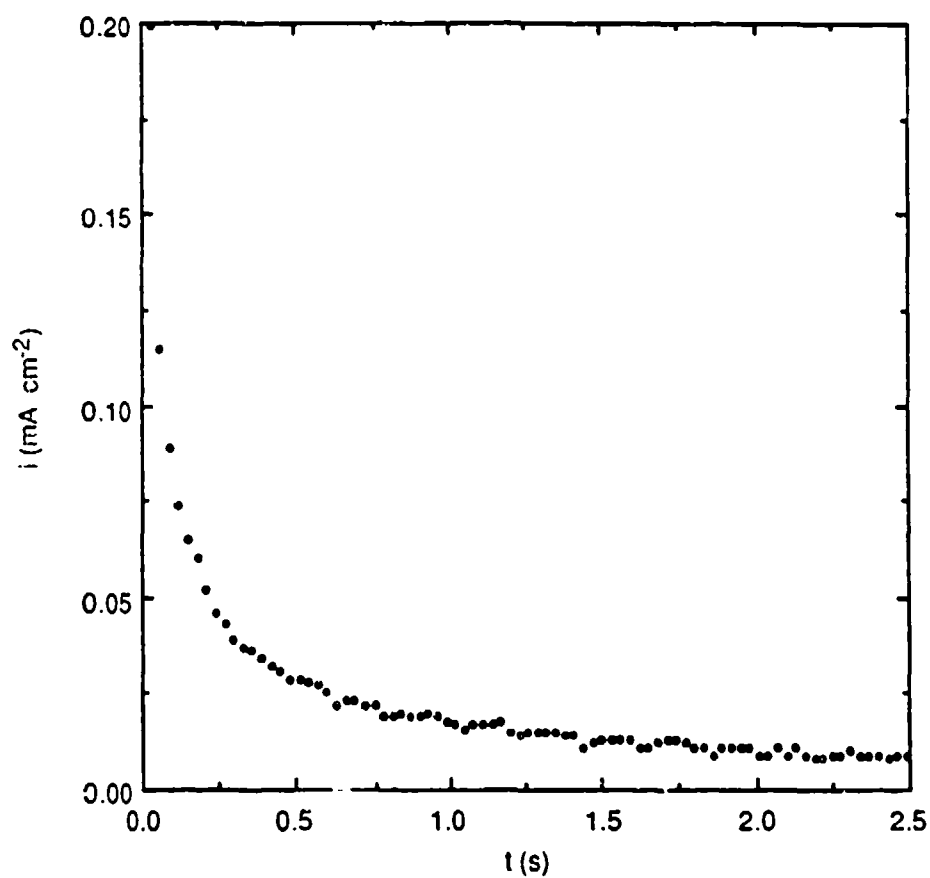
Figure 1. Anodic transient for titanium grade 2 in acetate buffer.
t_c = 15 s; E_c = -0.742 V (SCE).
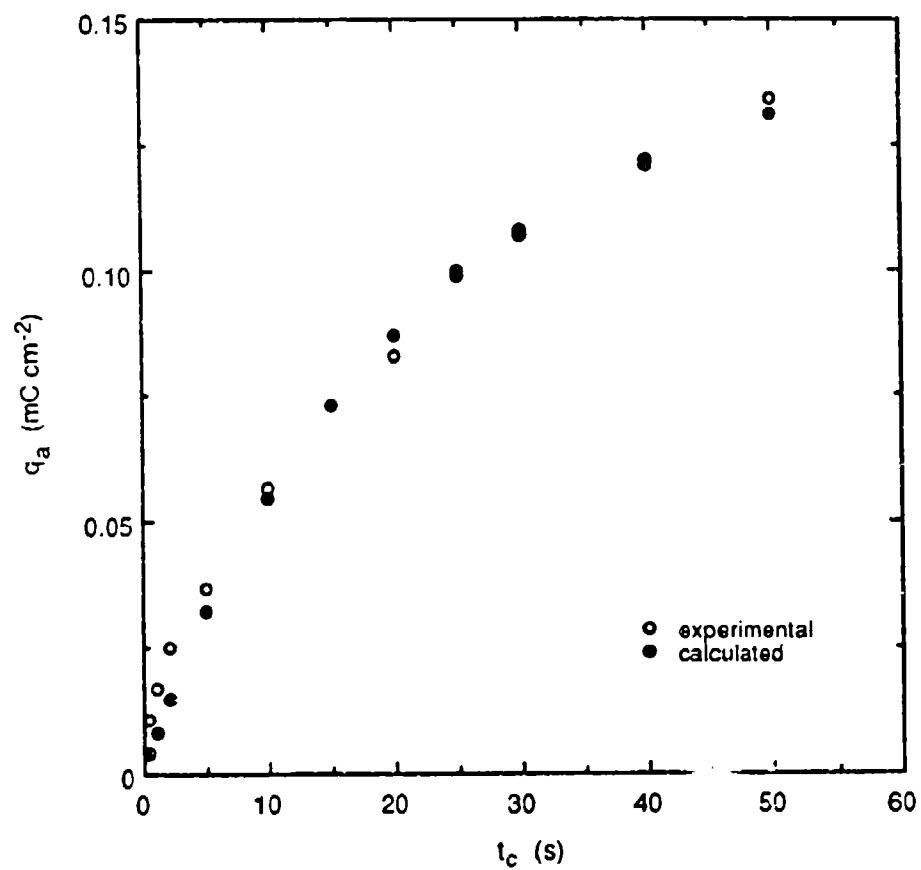
The full transient is not shown.

Figure 2. Comparison of experimental and calculated anodic charge data for titanium grade 2 in acetate buffer.
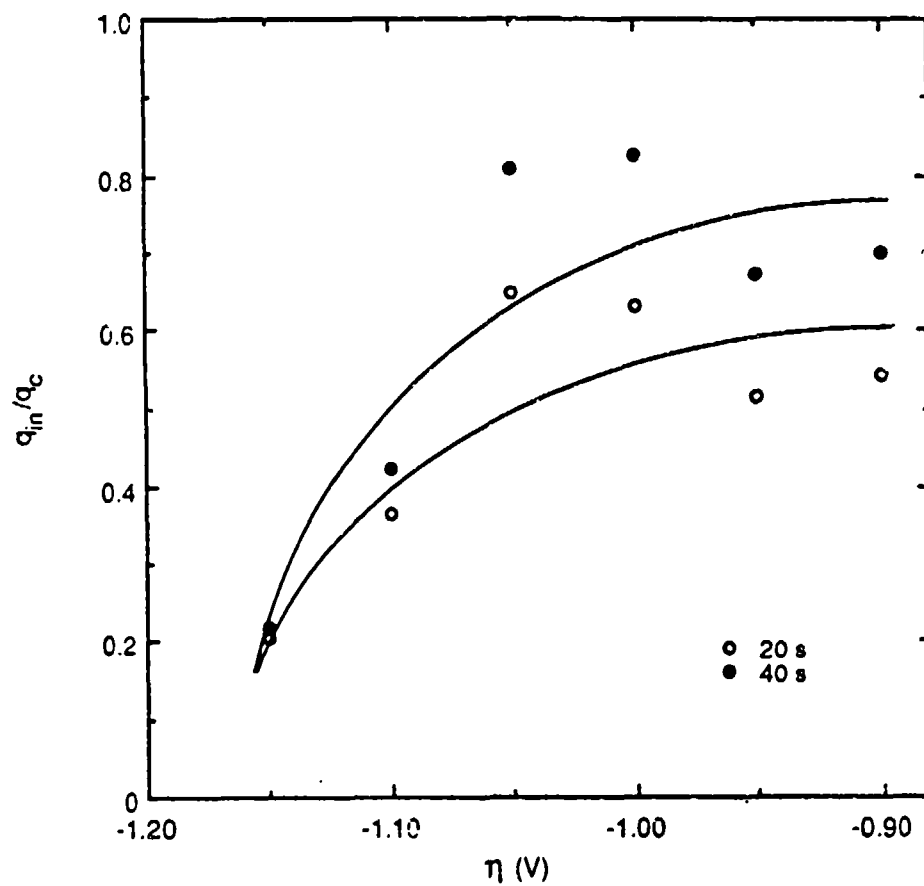
$E_c = -0.741$ V (SCE).

Figure 3. Dependence of q_{in}/q_c on overpotential for titanium grade 2 at high overpotentials and charging times of 20 s and 40 s.